Supplement of The Cryosphere, 13, 2537–2556, 2019
https://doi.org/10.5194/tc-13-2537-2019-supplement

The Cryosphere Open Access EGU

Supplement of

Changes of the tropical glaciers throughout Peru between 2000 and 2016 – mass balance and area fluctuations

Thorsten Seehaus et al.

Correspondence to: Thorsten Seehaus (thorsten.seehaus@fau.de)

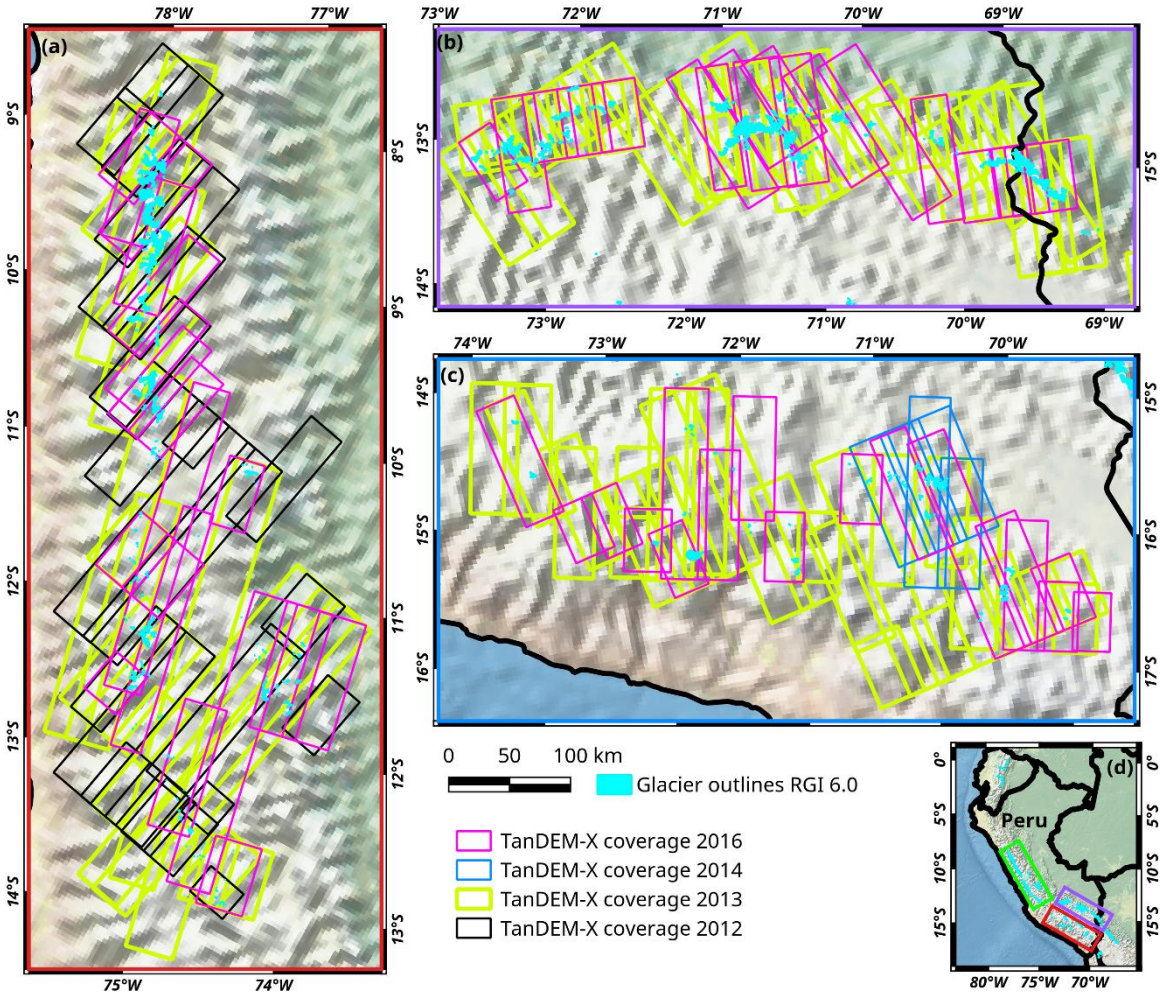

Figure S1. Coverage of the studied areas by TanDEM-X data. Panels (a-c): glacier subregions in Peru according to Sagredo and Lowell (2012); (a) subregion R1: northern wet outer tropics; (b) subregion R2: southern wet outer tropics; (c) subregion R3: dry outer tropics. Panel (d): overview map of Peru. Coloured rectangles indicate the locations of the subregions (same frame colours). Light blue areas: glacier coverage based on RGI 6.0. © Natural Earth

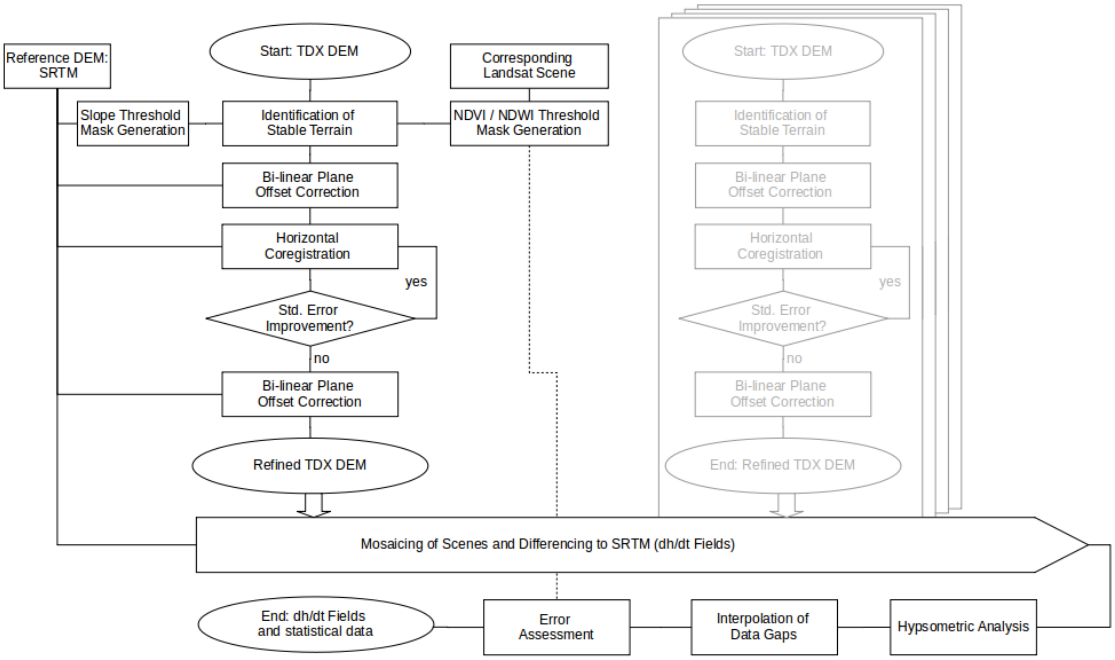

Figure S2. Flow chart of processing chain to perform coregistration, mosaicking, gap filling and error evaluation of TanDEM-X DEMs

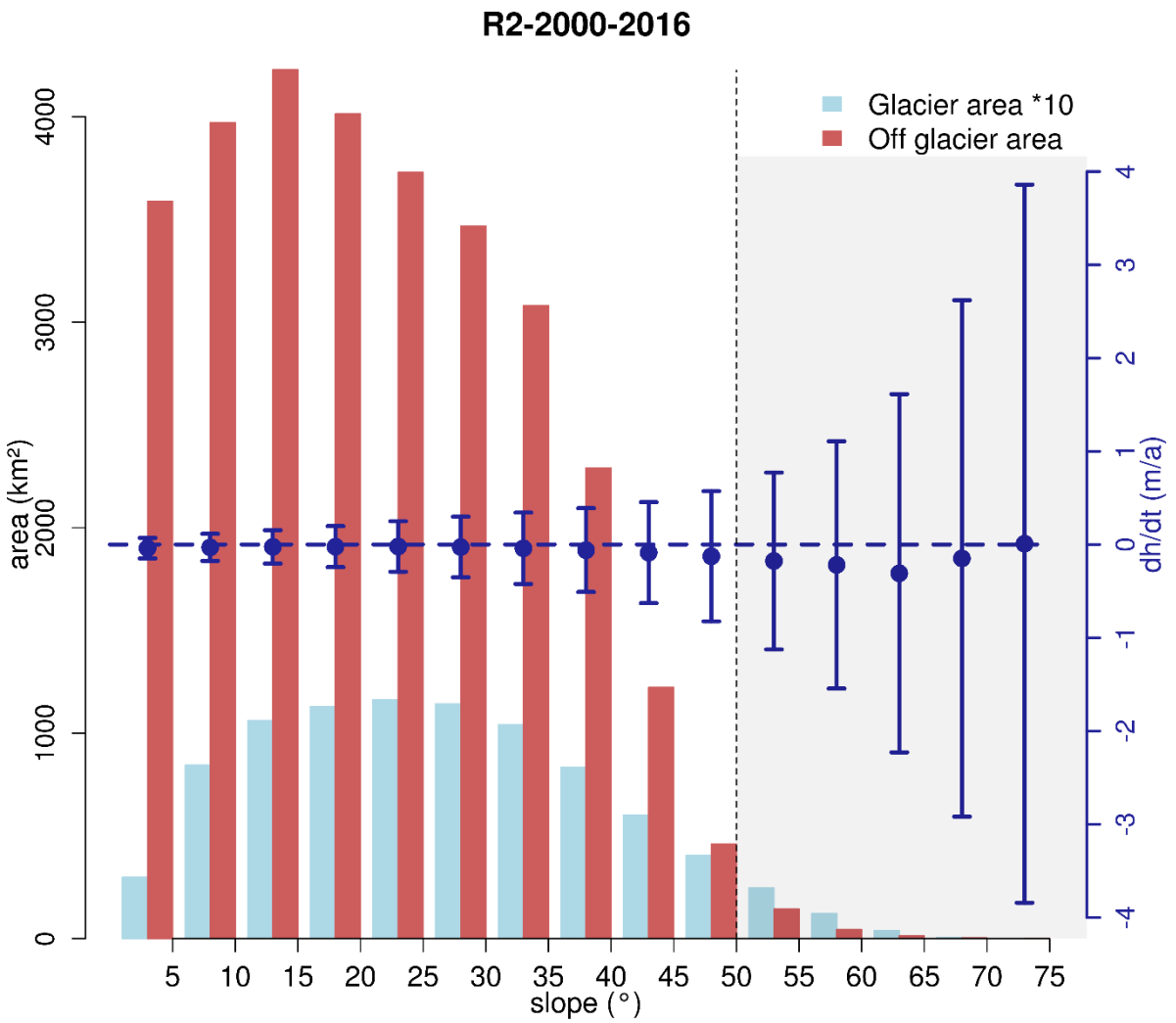

Figure S3. Off-(red) and on-glacier (light blue) area and off-glacier elevation change (blue dots) distributions in dependency on slope in subregion R2 for the period 2000-2016. Error bars represent NMAD of Δh/Δt values in the individual slope interval. Dotted line indicates the applied slope threshold (see Section 4.2). Glacier area measurements are based on the glacier outlines from 2000. Note: For better representation, on-glacier areas are scaled by a factor of 10.

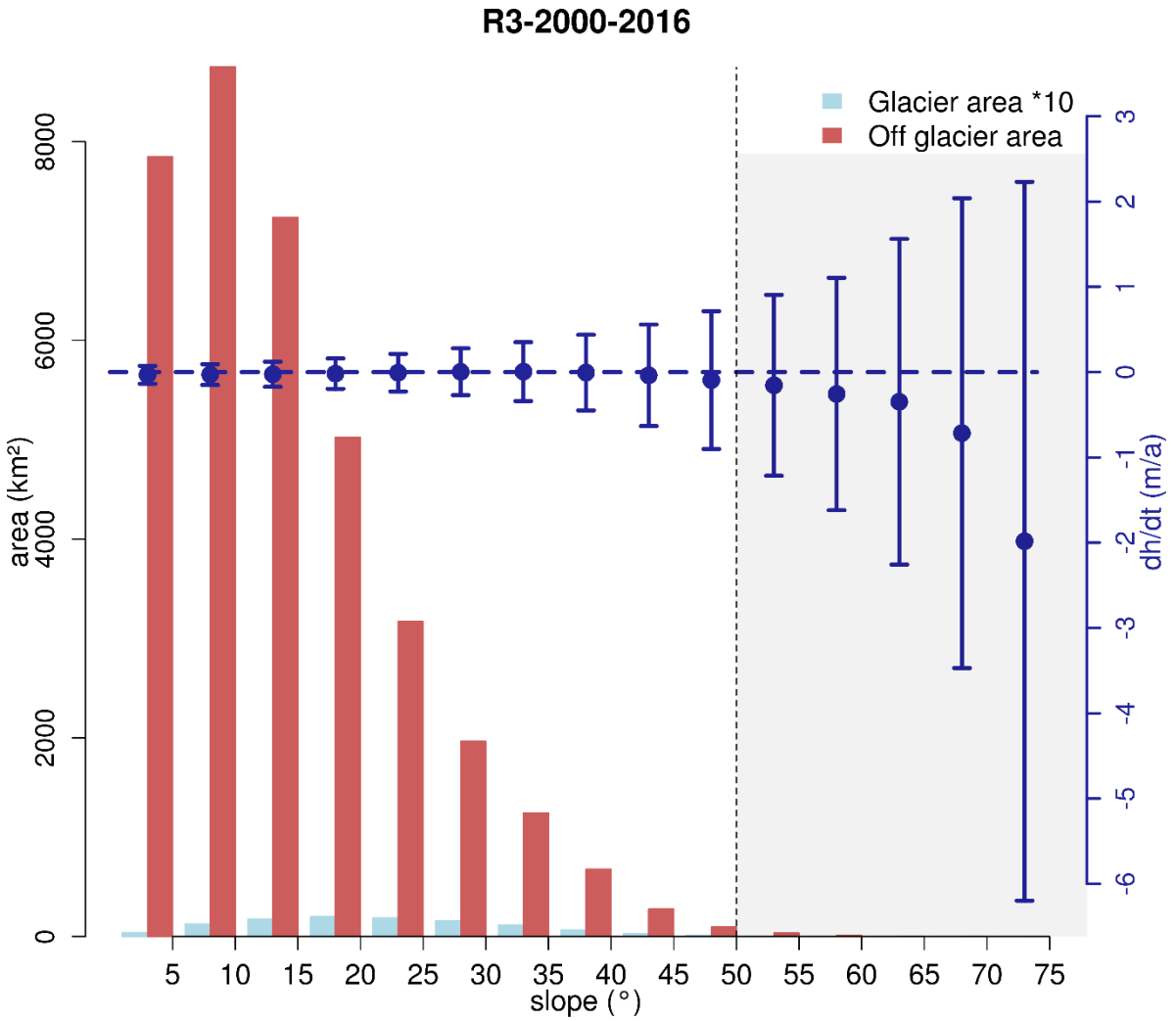

Figure S4. Off-(red) and on-glacier (light blue) area and off-glacier elevation change (blue dots) distributions in dependency on slope in subregion R3 for the period 2000-2016. Error bars represent NMAD of Δh/Δt values in the individual slope interval. Dotted line indicates the applied slope threshold (see Section 4.2). Glacier area measurements are based on the glacier outlines from 2000. Note: For better representation, on-glacier areas are scaled by a factor of 10.

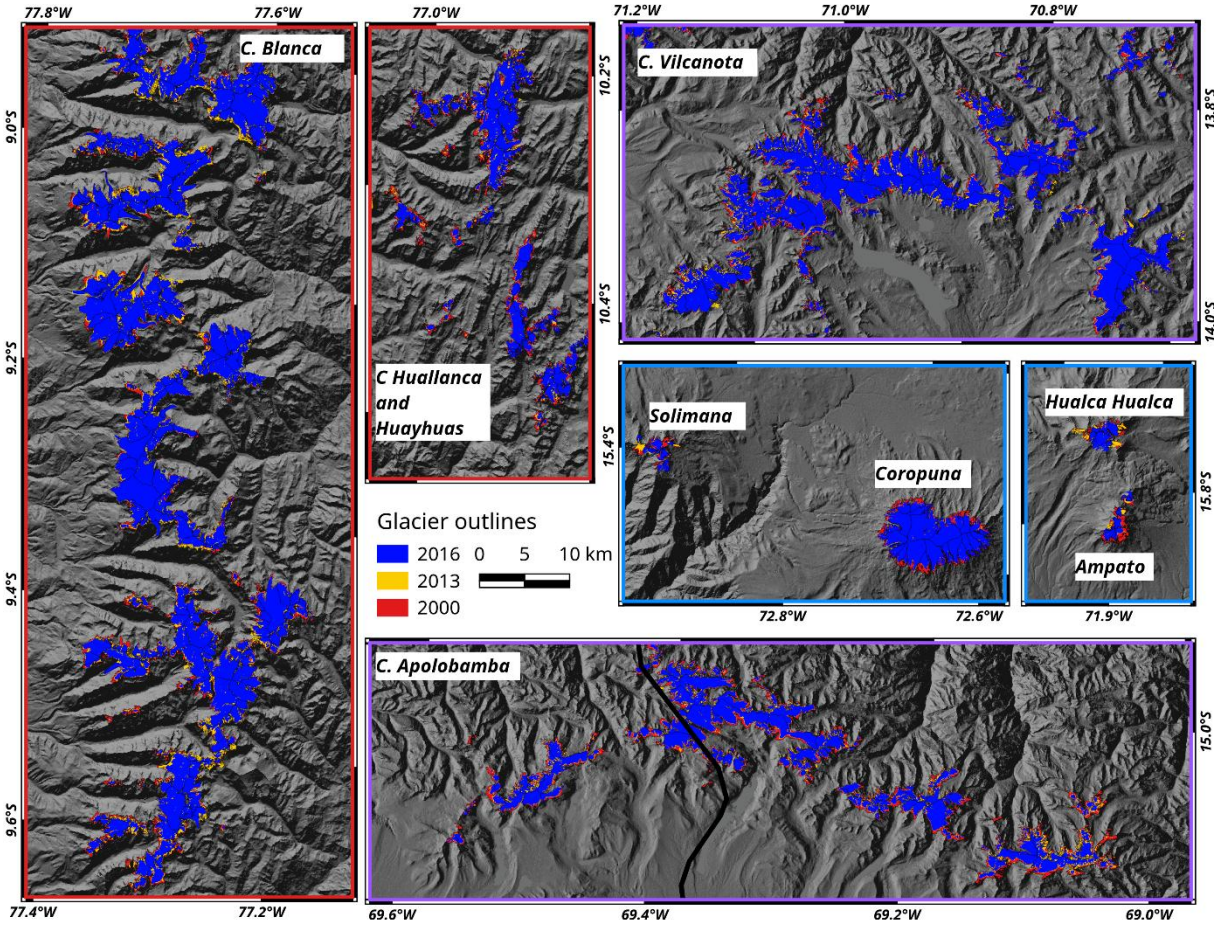

Figure S5. Glacier outlines at example mountain ranges in all three subregions in the years 2000, 2013 and 2016. The frame colour of the panels indicates the subregions (see Figure 1, main manuscript). Background: SRTM DEM hillshade © NASA

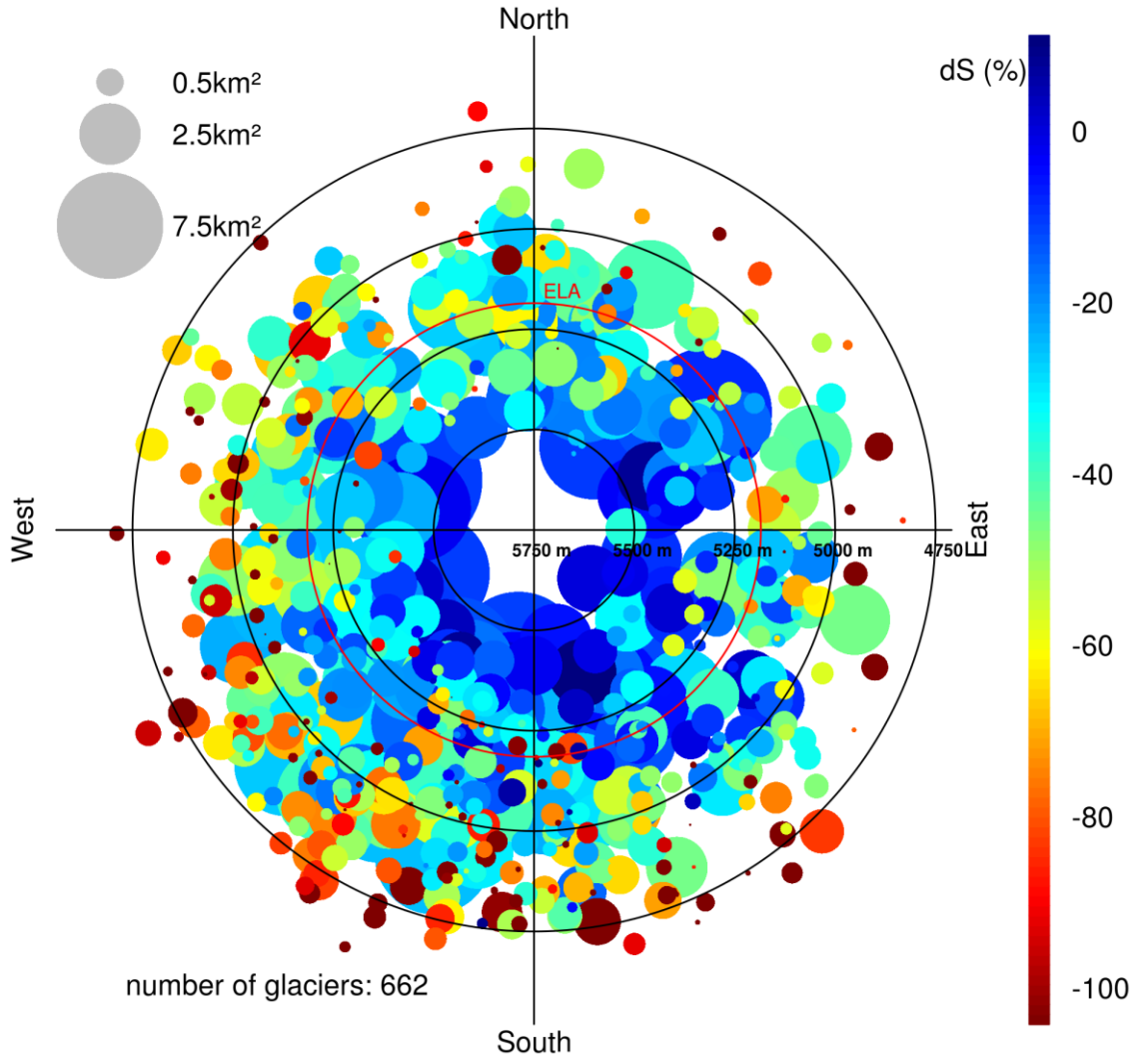

Figure S6. Polar plot of relative area changes (dot colour) in subregion R2 in the period 2000-2016 of individual glaciers. Dot size: glacier size in 2000; Radius: median elevation; Orientation: mean aspect. Red circle: equilibrium line altitude (ELA), see also Table S3.

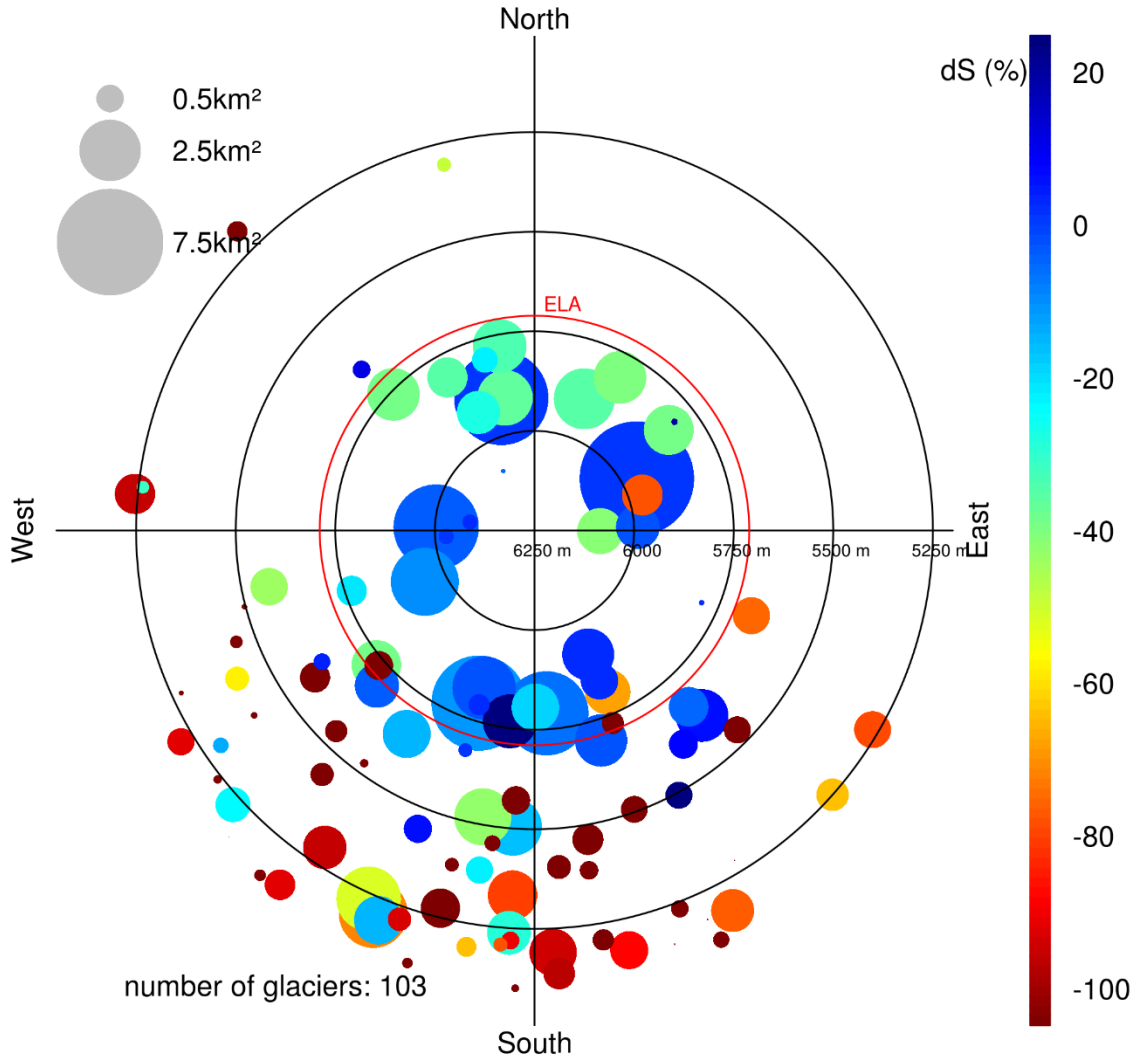

Figure S7. Polar plot of relative area changes (dot colour) in subregion R3 in the period 2000-2016 of individual glaciers. Dot size: glacier size in 2000; Radius: median elevation; Orientation: mean aspect. Red circle: equilibrium line altitude (ELA), see also Table S3.

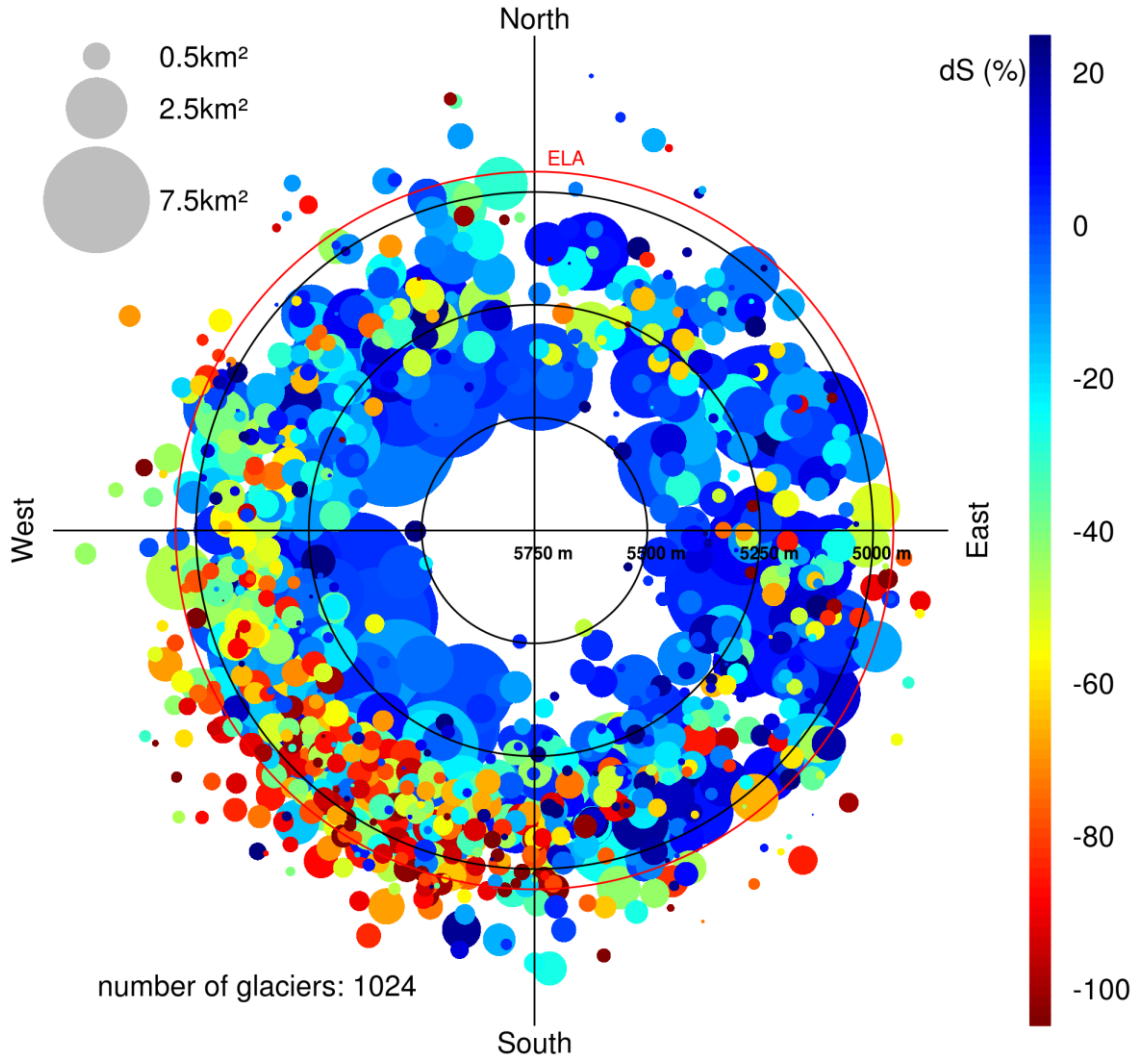

Figure S8. Polar plot of relative area changes (dot colour) in subregion R1 in the period 2000-2013 of individual glaciers. Dot size: glacier size in 2000; Radius: median elevation; Orientation: mean aspect. Red circle: equilibrium line altitude (ELA), see also Table S3.

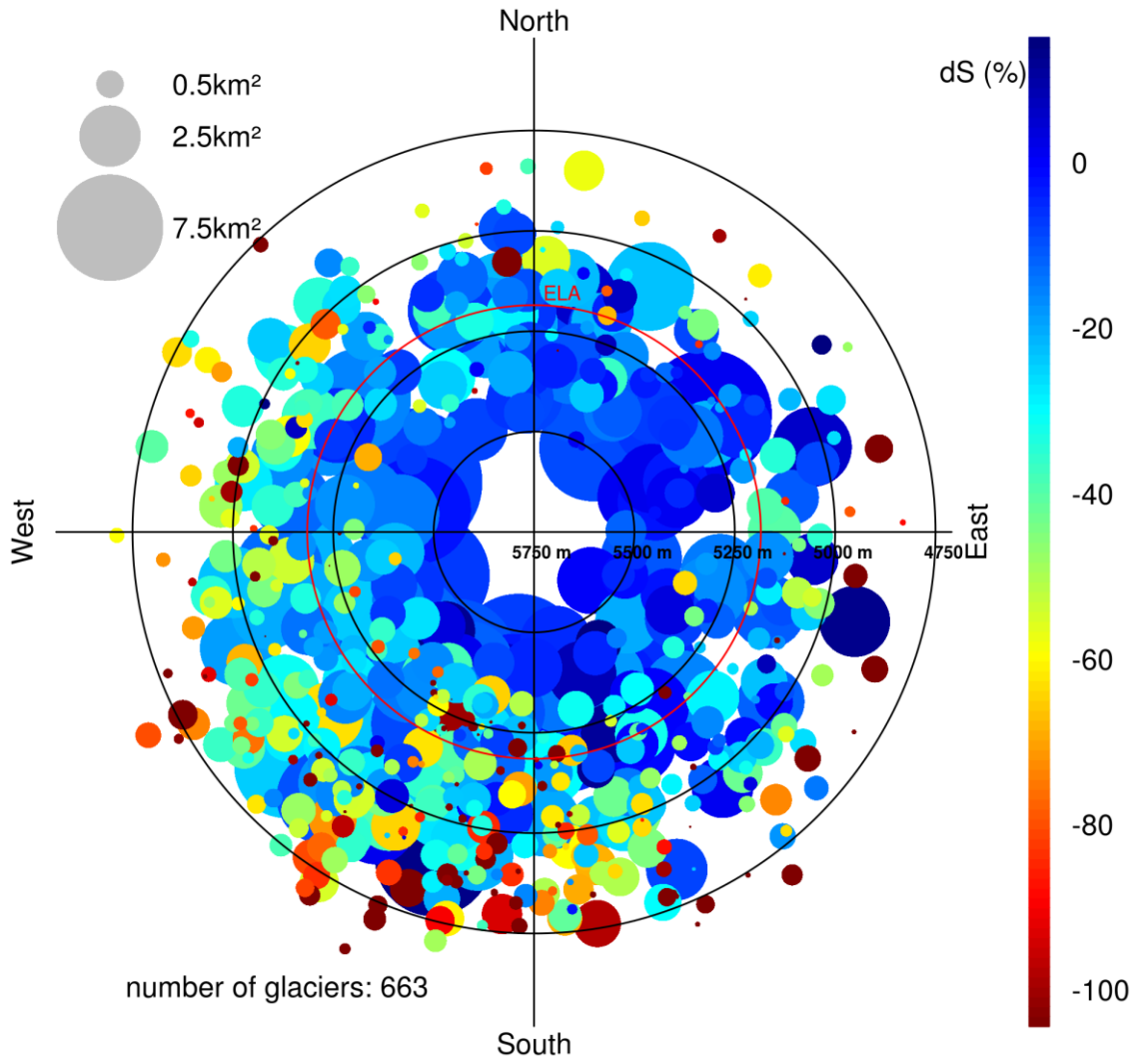

Figure S9. Polar plot of relative area changes (dot colour) in subregion R2 in the period 2000-2013 of individual glaciers. Dot size: glacier size in 2000; Radius: median elevation; Orientation: mean aspect. Red circle: equilibrium line altitude (ELA), see also Table S3.

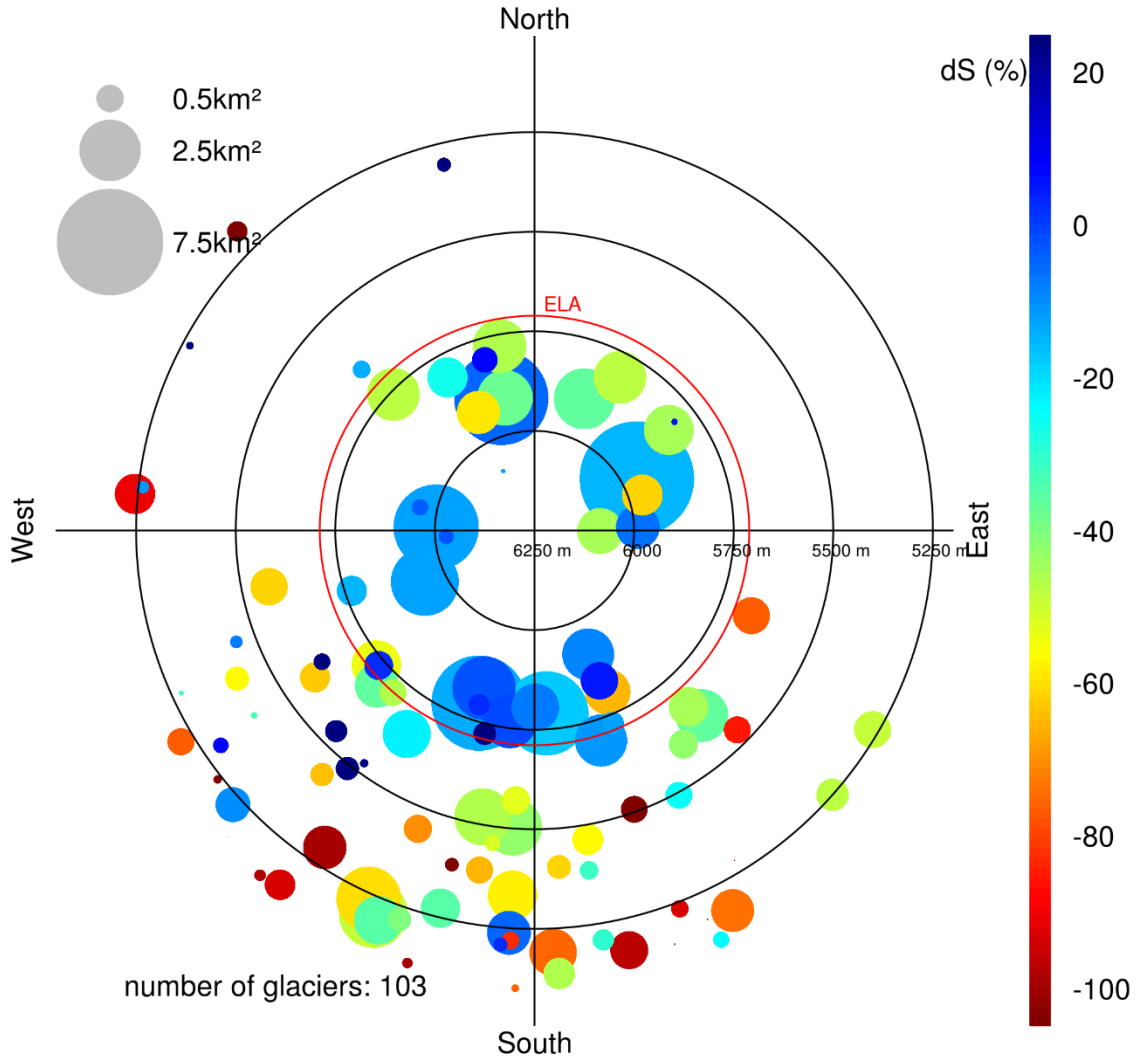

Figure S10. Polar plot of relative area changes (dot colour) in subregion R3 in the period 2000-2013 of individual glaciers. Dot size: glacier size in 2000; Radius: median elevation; Orientation: mean aspect. Red circle: equilibrium line altitude (ELA), see also Table S3.

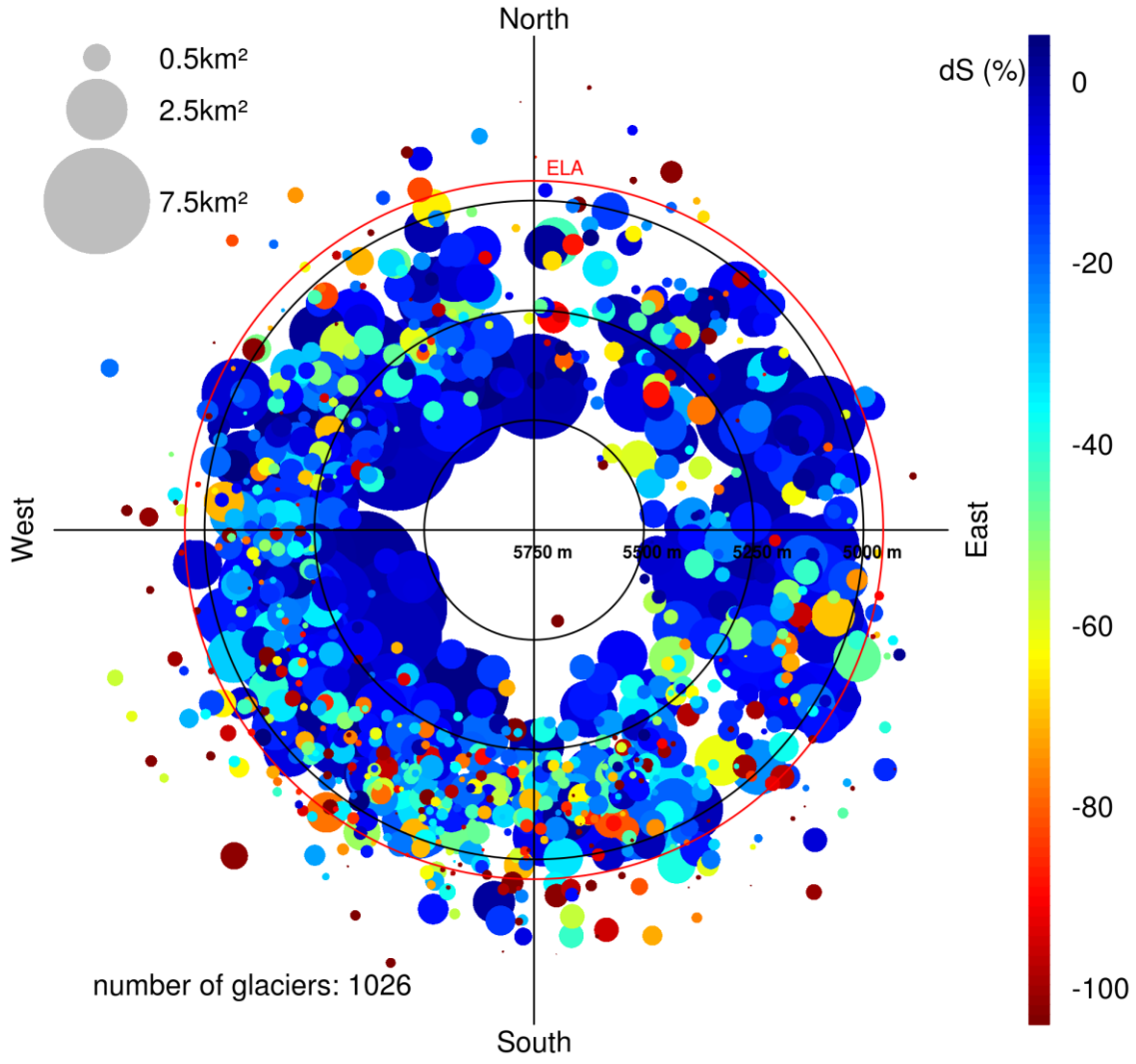

Figure S11. Polar plot of relative area changes (dot colour) in subregion R1 in the period 2013-2016 of individual glaciers. Dot size: glacier size in 2013; Radius: median elevation; Orientation: mean aspect. Red circle: equilibrium line altitude (ELA), see also Table S3.

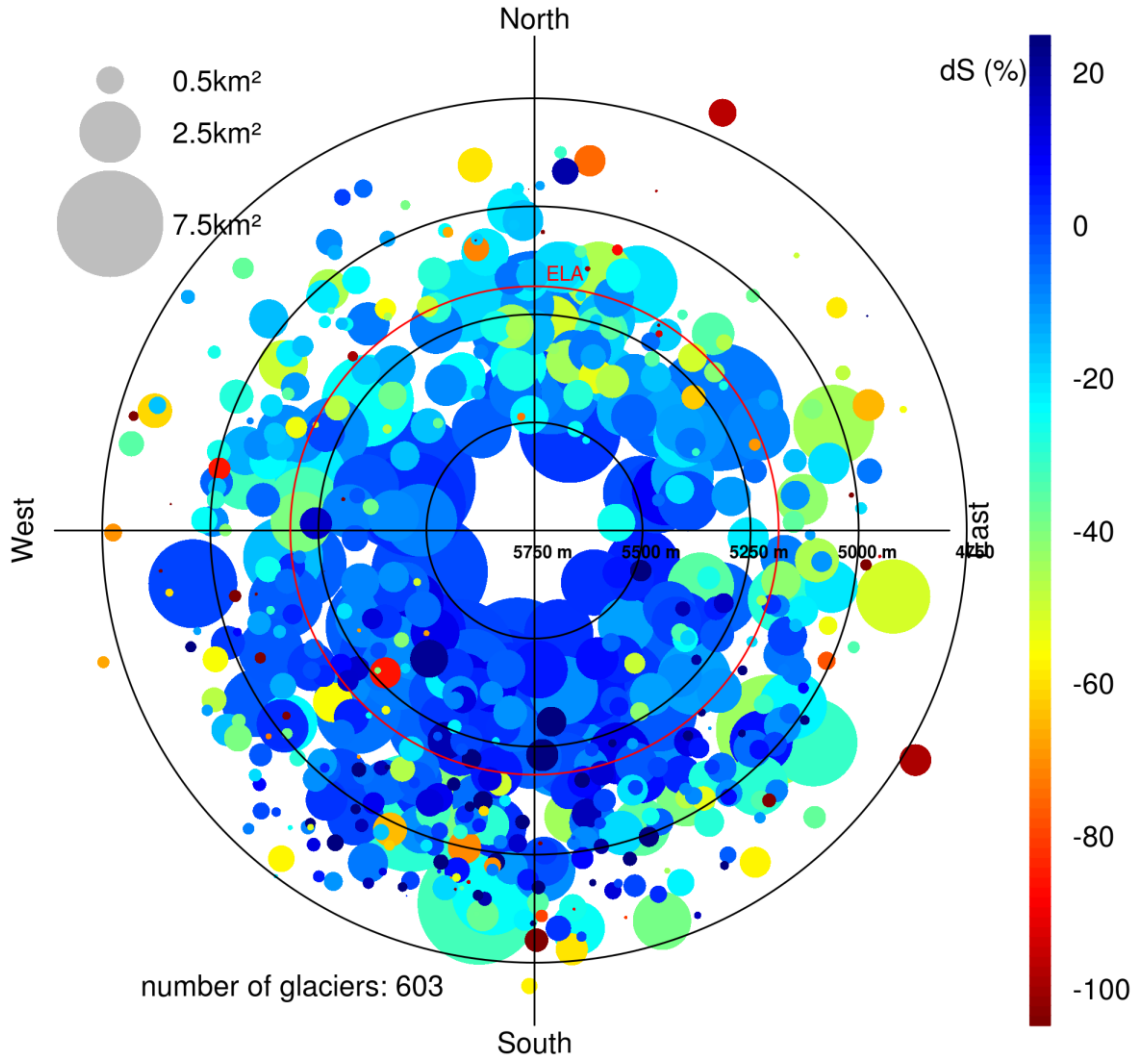

Figure S12. Polar plot of relative area changes (dot colour) in subregion R2 in the period 2013-2016 of individual glaciers. Dot size: glacier size in 2013; Radius: median elevation; Orientation: mean aspect. Red circle: equilibrium line altitude (ELA), see also Table S3.

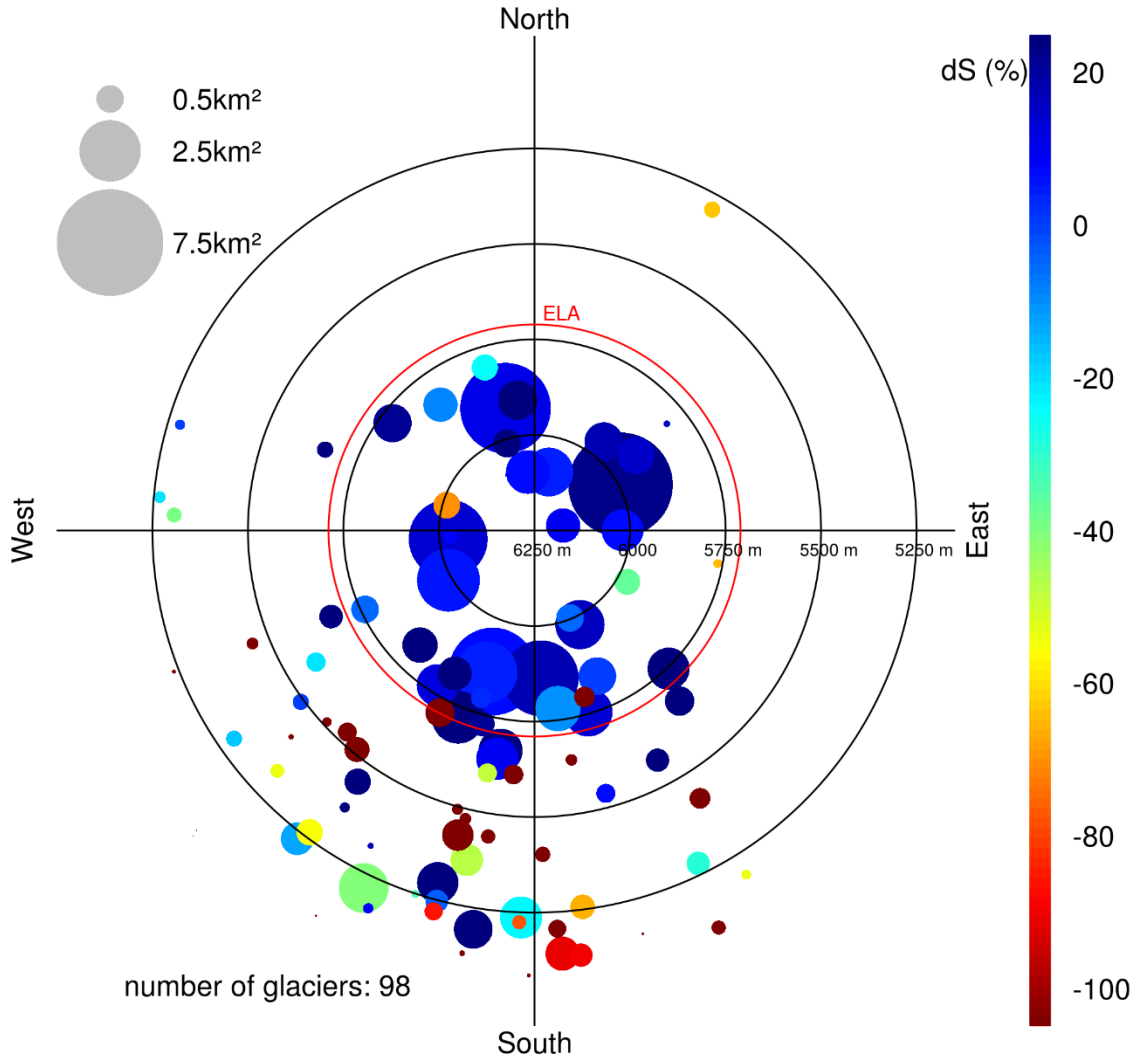

Figure S13. Polar plot of relative area changes (dot colour) in subregion R3 in the period 2013-2016 of individual glaciers. Dot size: glacier size in 2013; Radius: median elevation; Orientation: mean aspect. Red circle: equilibrium line altitude (ELA), see also Table S3.

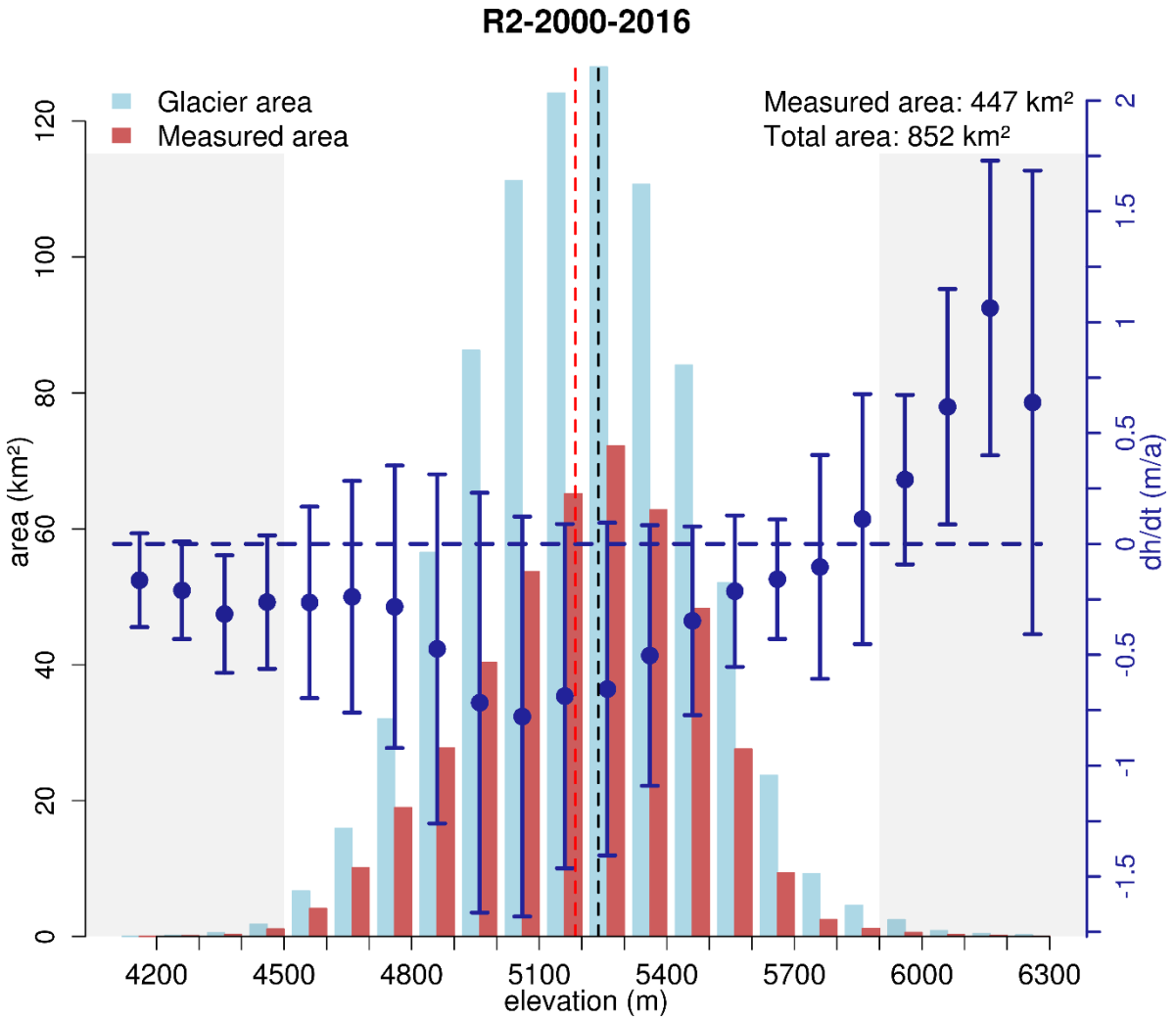

Figure S14. Hypsometric distribution of measured (red bars) and total (light blue bars) glacier area with elevation in subregion R2 in the interval 2000-2016. Blue dots represent the mean Δh/Δt value in each elevation interval. Error bars indicate NMAD of Δh/Δt for each hypsometric bin. Grey areas mark the lower and upper 1% quantile of the glacier area distribution. Black dashed line: mean glacier elevation; Red dashed line: equilibrium line altitude (ELA), see also Table S3. Area measurements are based on the glacier outlines from 2000, considering only regions with slopes below applied slope threshold (50°, see Section 4.2)

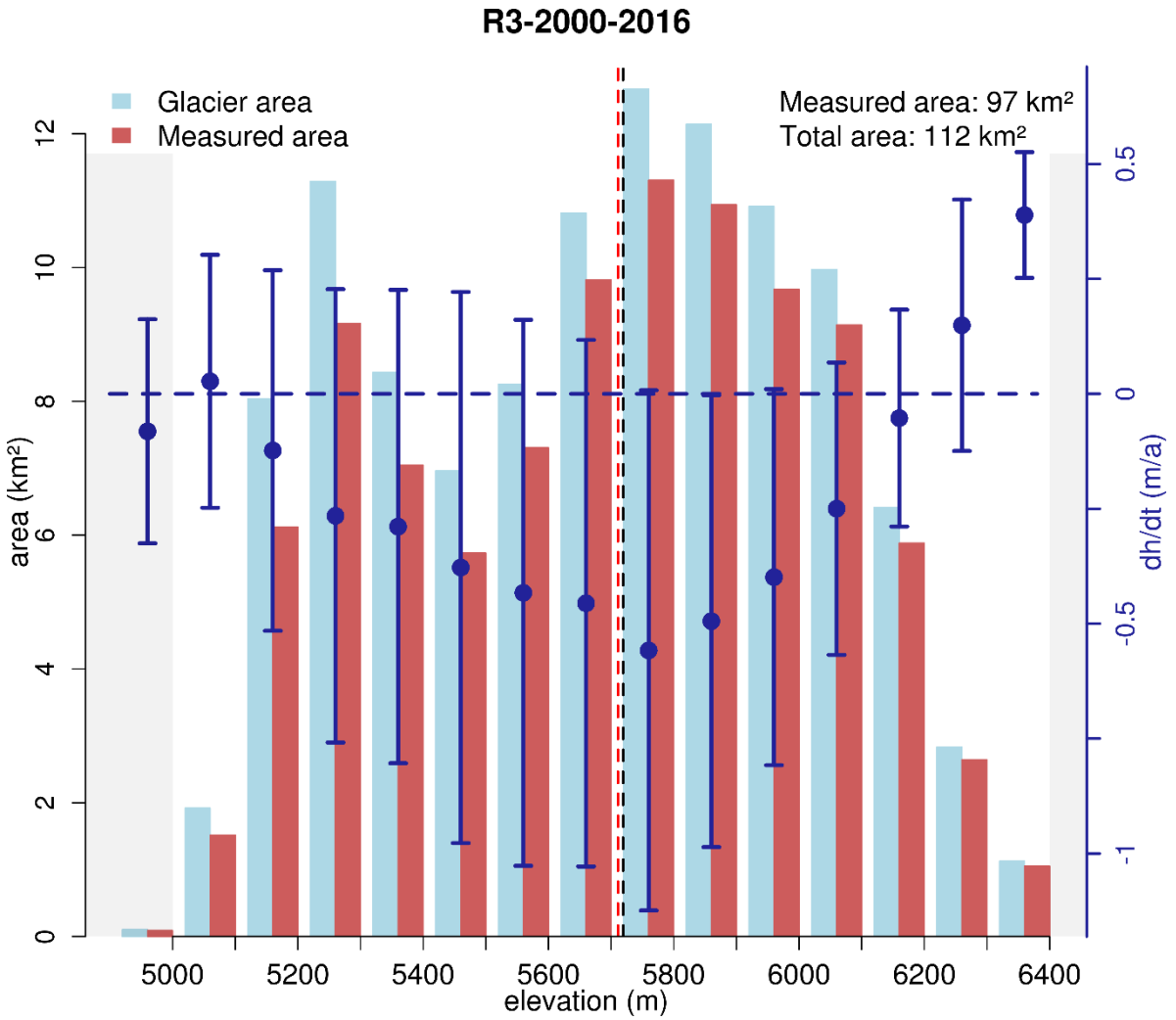

Figure S15. Hypsometric distribution of measured (red bars) and total (light blue bars) glacier area with elevation in subregion R3 in the interval 2000-2016. Blue dots represent the mean Δh/Δt value in each elevation interval. Error bars indicate NMAD of Δh/Δt for each hypsometric bin. Grey areas mark the lower and upper 1% quantile of the glacier area distribution. Black dashed line: mean glacier elevation; Red dashed line: equilibrium line altitude (ELA), see also Table S3. Area measurements are based on the glacier outlines from 2000, considering only regions with slopes below applied slope threshold (50°, see Section 4.2)

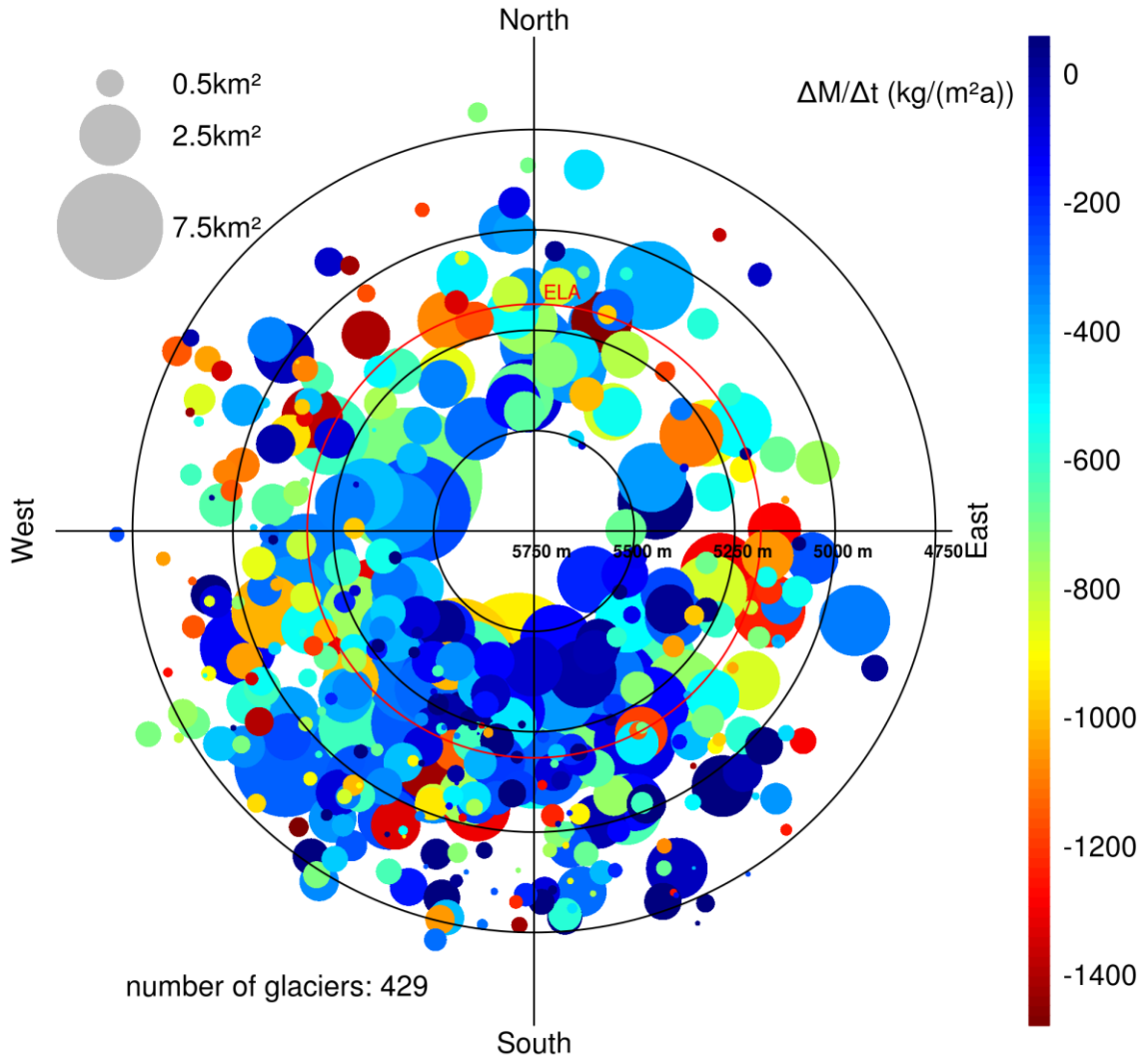

Figure S16. Polar plot of specific mass balance (dot colour) of individual glaciers in subregion R2 in the period 2000-2016 of individual glaciers. Dot size: glacier size in 2000; Radius: median elevation; Orientation: mean aspect. Red circle: equilibrium line altitude (ELA), see also Table S3. Note: only glaciers with elevation change information >50% are included.

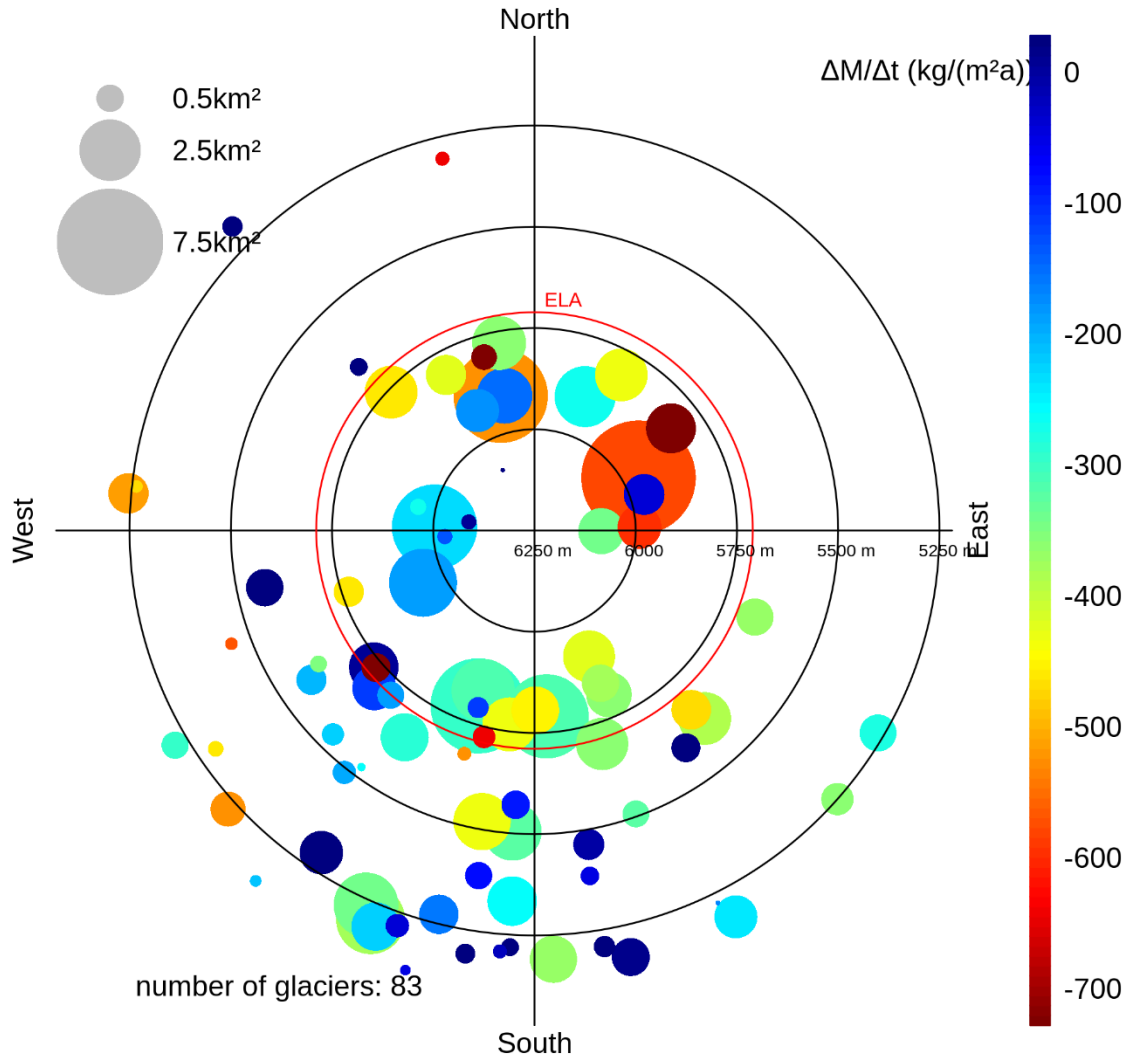

Figure S17. Polar plot of specific mass balance (dot colour) of individual glaciers in subregion R3 in the period 2000-2016 of individual glaciers. Dot size: glacier size in 2000; Radius: median elevation; Orientation: mean aspect. Red circle: equilibrium line altitude (ELA), see also Table S3. Note: only glaciers with elevation change information >50% are included.

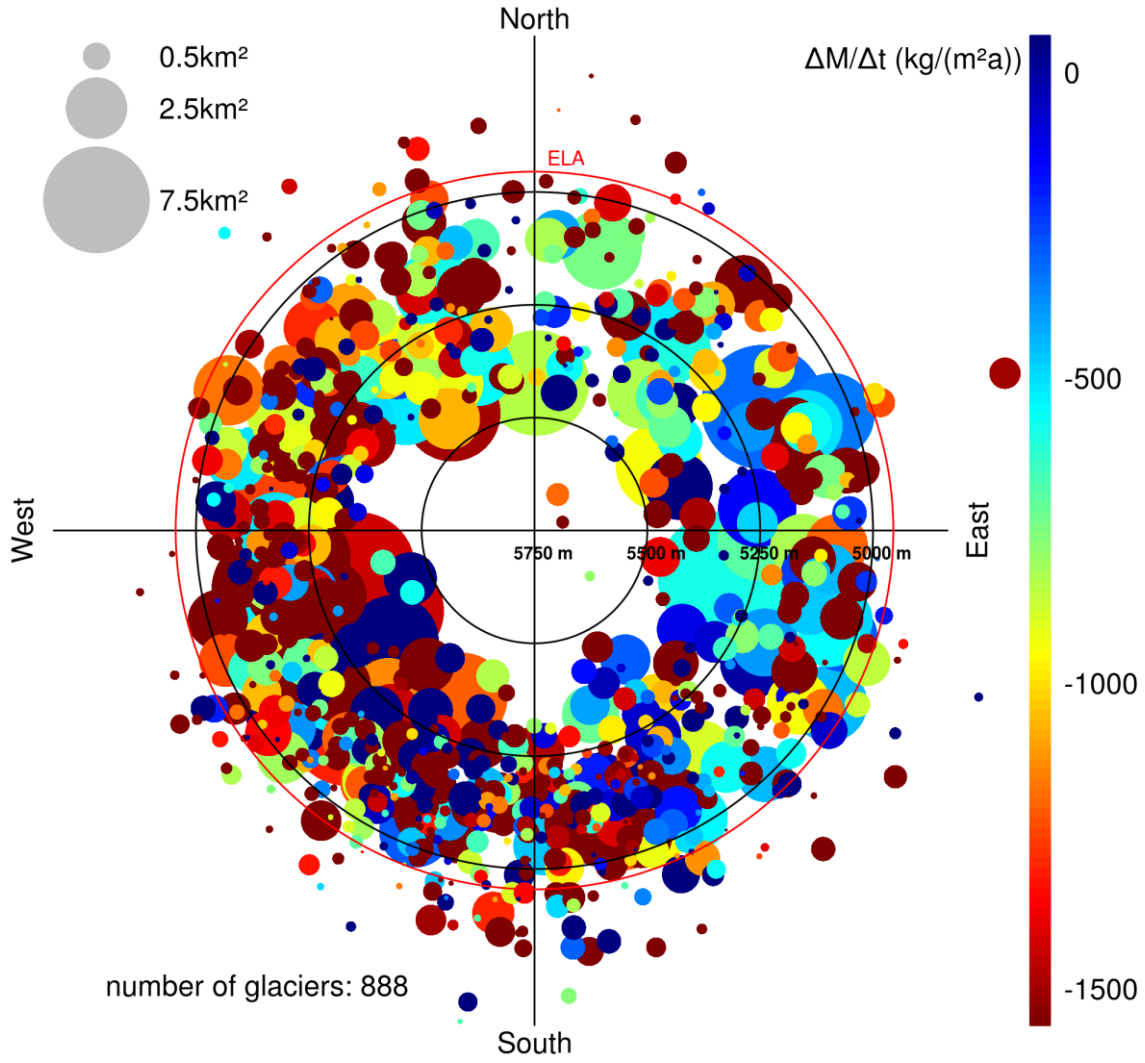

Figure S18. Polar plot of specific mass balance (dot colour) of individual glaciers in subregion R1 in the period 2013-2016 of individual glaciers. Dot size: glacier size in 2013; Radius: median elevation; Orientation: mean aspect. Red circle: equilibrium line altitude (ELA), see also Table S3. Note: only glaciers with elevation change information >50% are included.

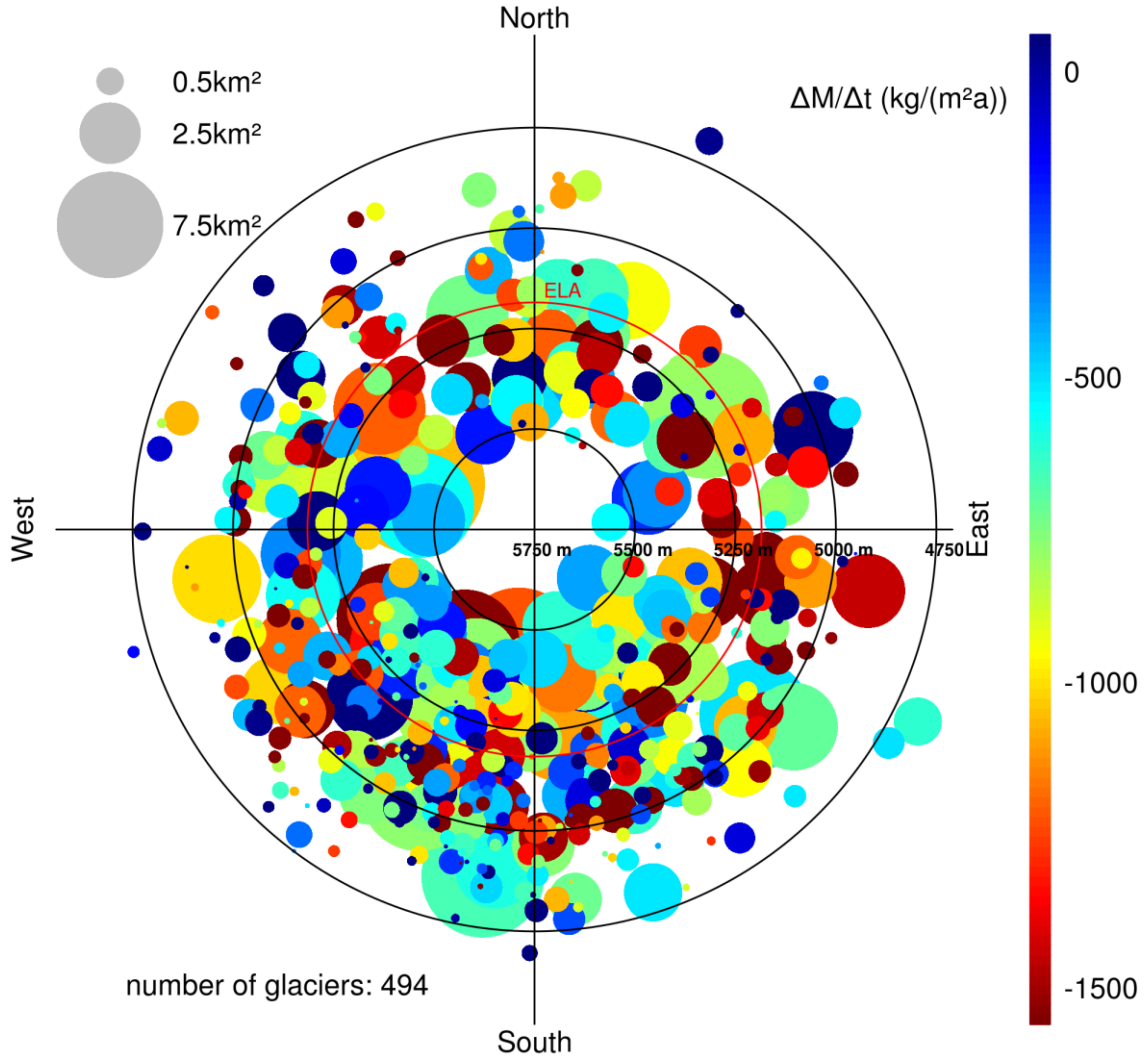

Figure S19. Polar plot of specific mass balance (dot colour) of individual glaciers in subregion R2 in the period 2013-2016 of individual glaciers. Dot size: glacier size in 2013; Radius: median elevation; Orientation: mean aspect. Red circle: equilibrium line altitude (ELA), see also Table S3. Note: only glaciers with elevation change information >50% are included.

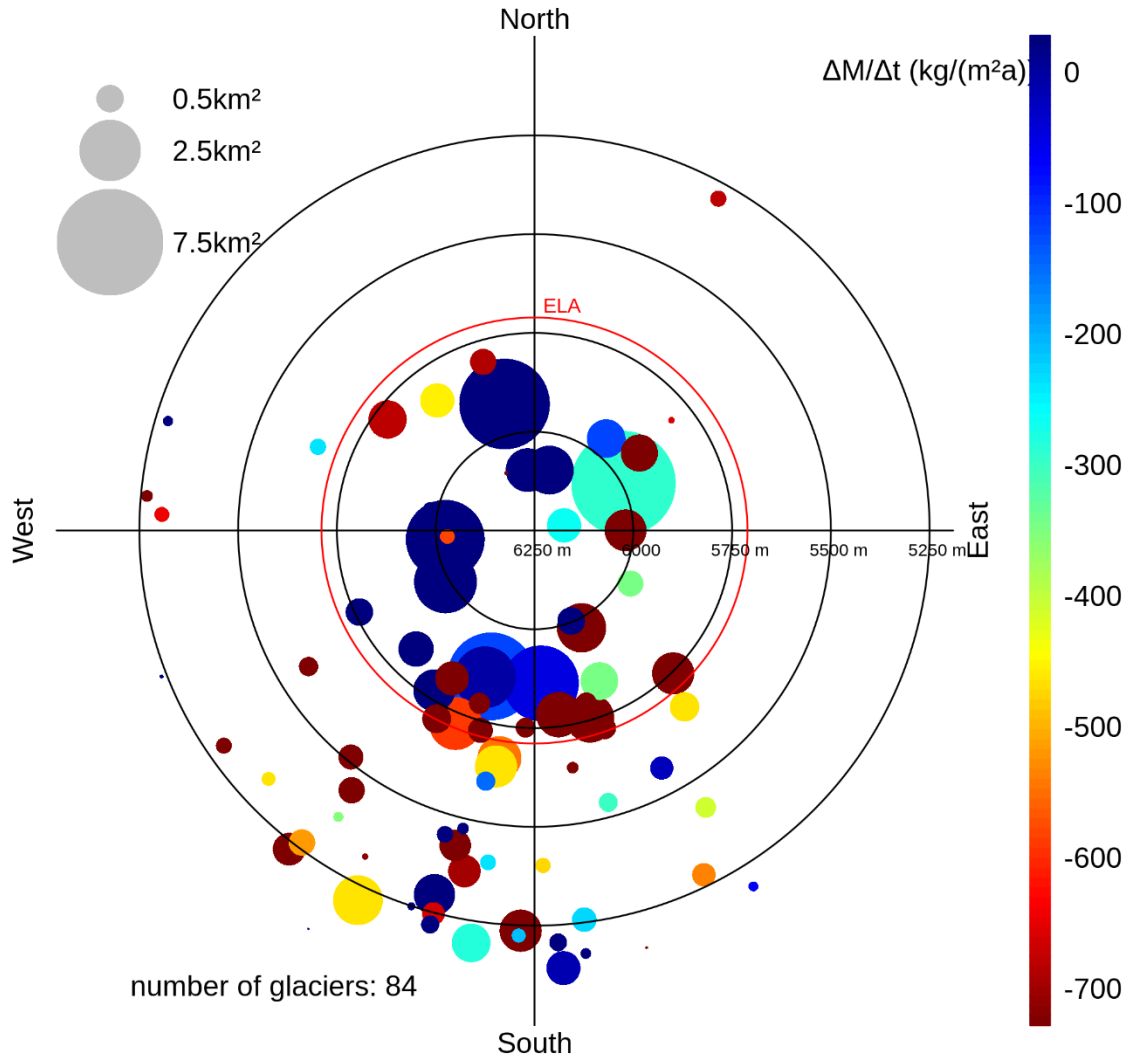

Figure S20. Polar plot of specific mass balance (dot colour) of individual glaciers in subregion R3 in the period 2013-2016 of individual glaciers. Dot size: glacier size in 2013; Radius: median elevation; Orientation: mean aspect. Red circle: equilibrium line altitude (ELA), see also Table S3. Note: only glaciers with elevation change information >50% are included.

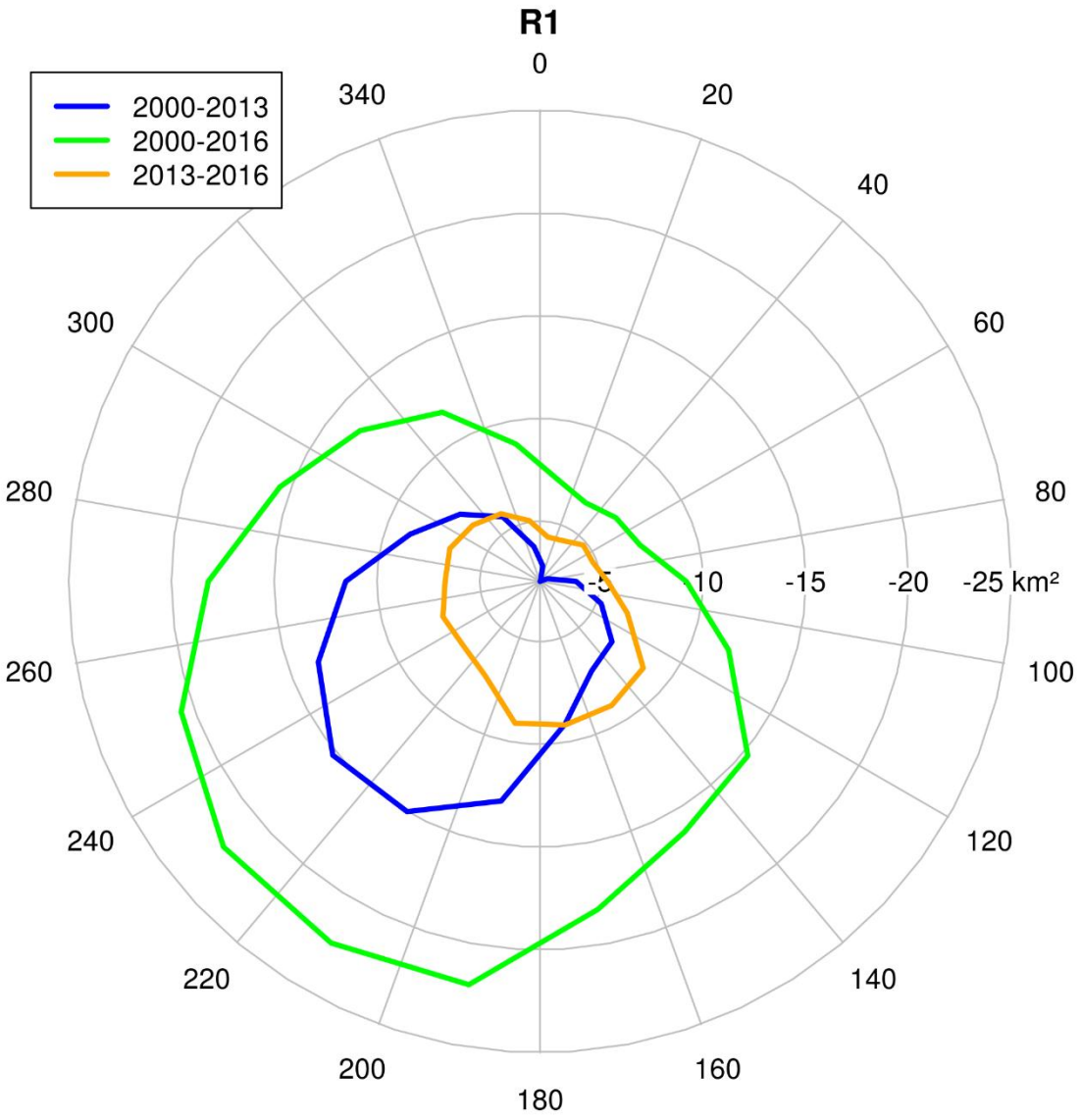

Figure S21. Polar plot of glacier area loss in subregion R1. The area losses are binned in aspect intervals of 20°.

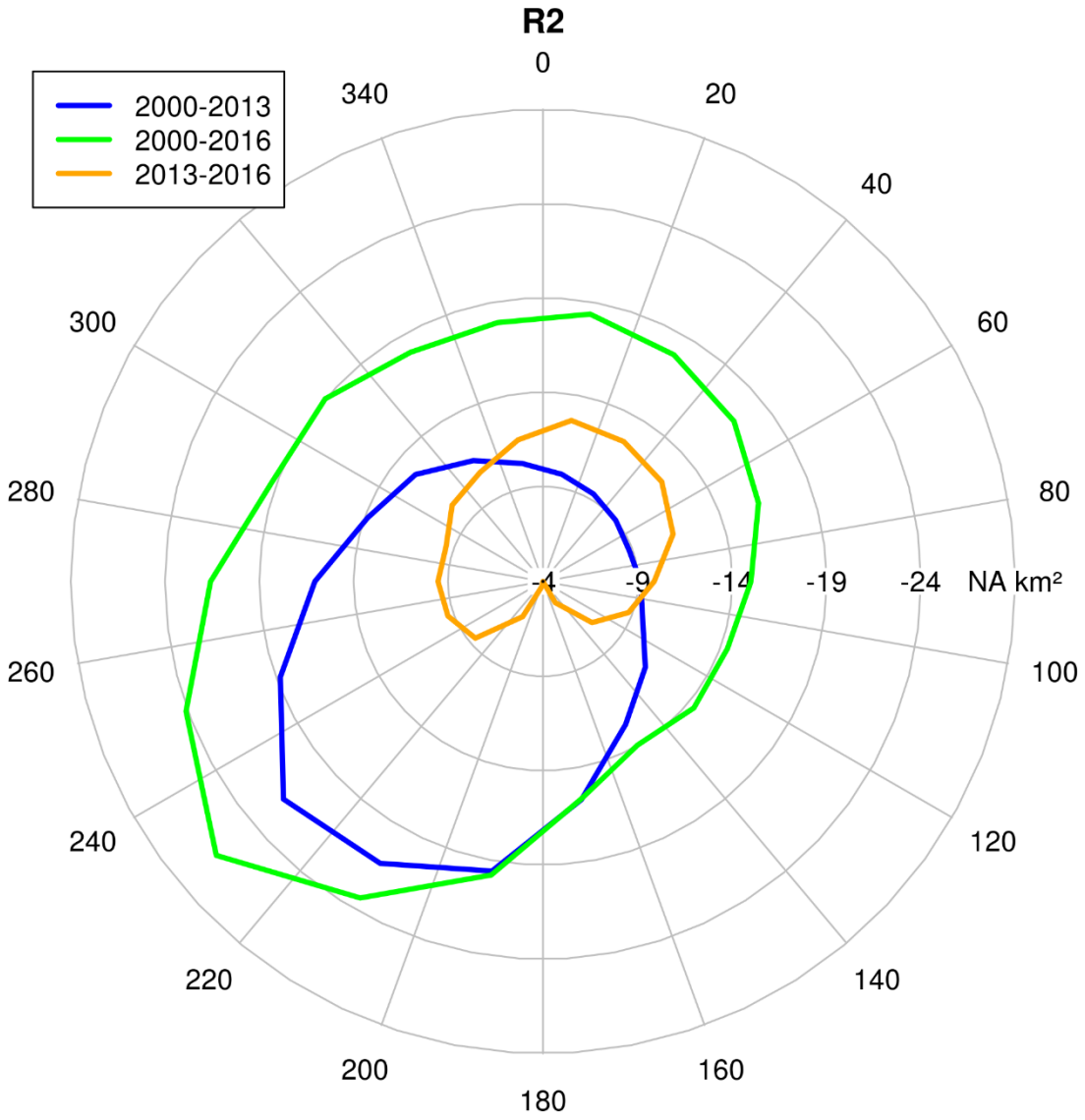

Figure S22. Polar plot of glacier area loss in subregion R2. The area losses are binned in aspect intervals of 20°.

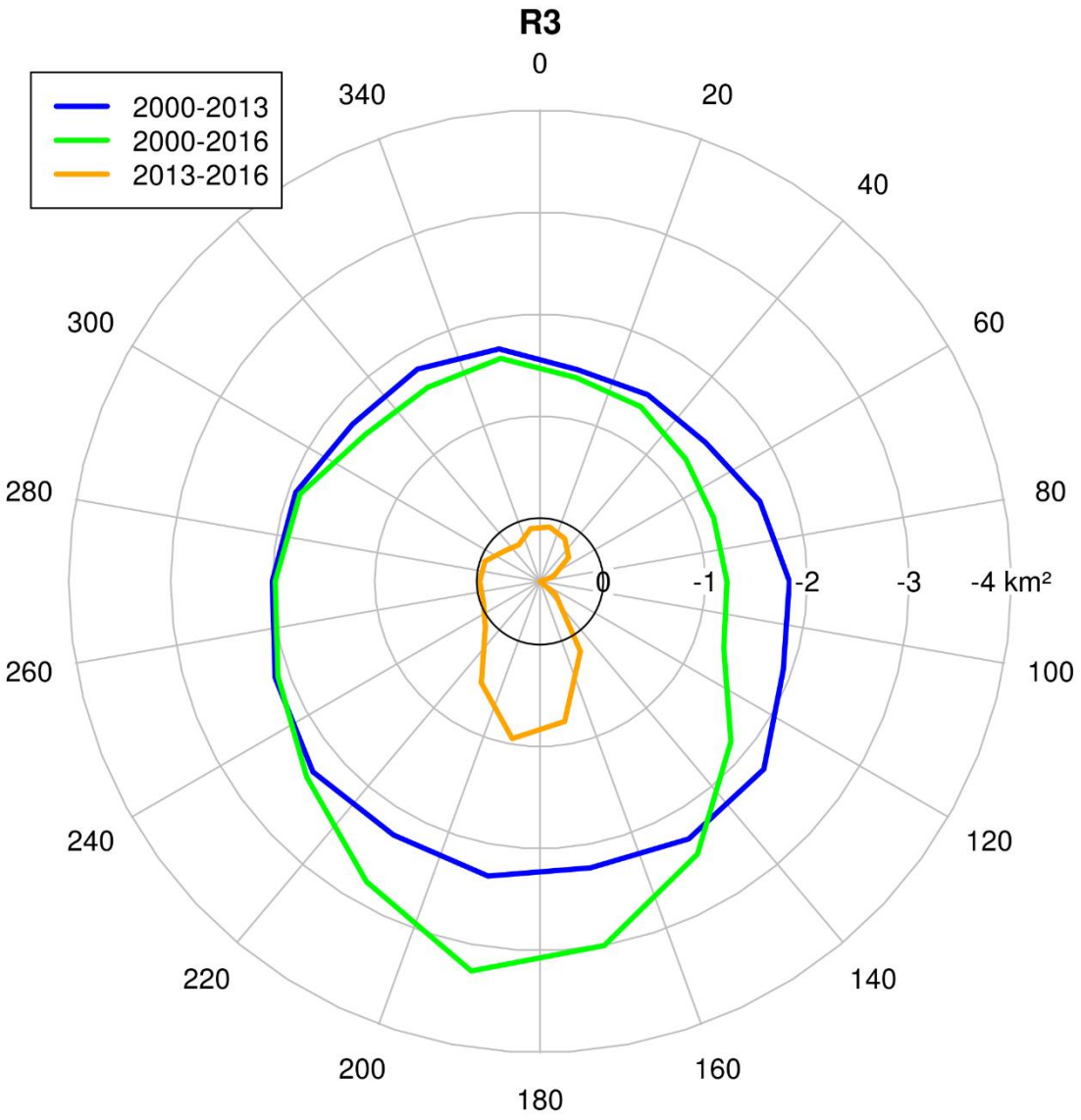

Figure S23. Polar plot of glacier area loss in subregion R3. The area losses are binned in aspect intervals of 20°.

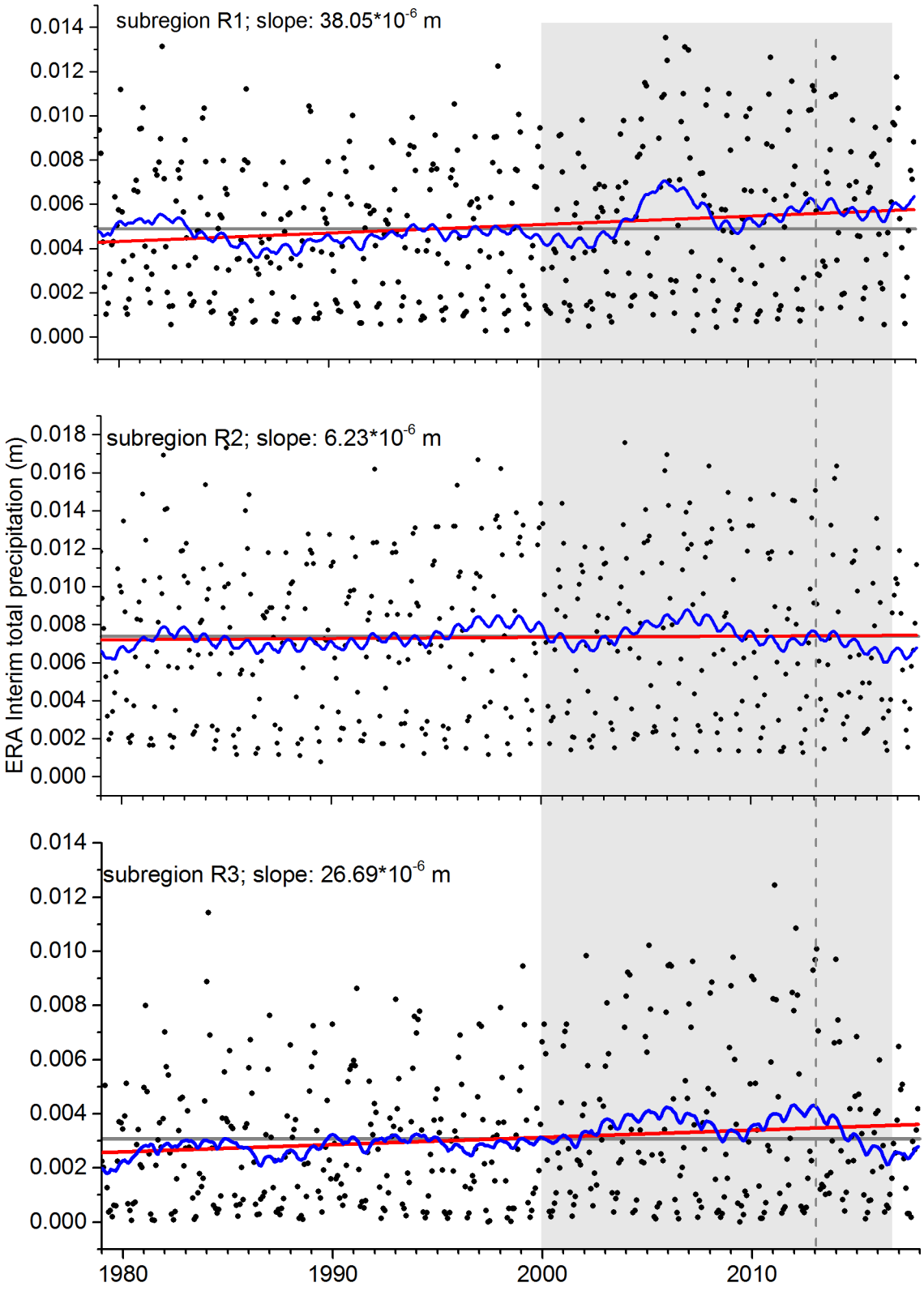

Figure S24. Total precipitation (monthly means of daily forecast accumulations) in the period 1979-2017 derived from ERA-Interim reanalysis data. Black dots: Spatial average values of glacier covered ERA-Interim grid cells in each subregion. Red line: long term trend (1979-2017), grey line: long term mean value; grey shaded area: period of mass budget and area change analysis, dashed grey line: marker for intermediate time step (early 2013)

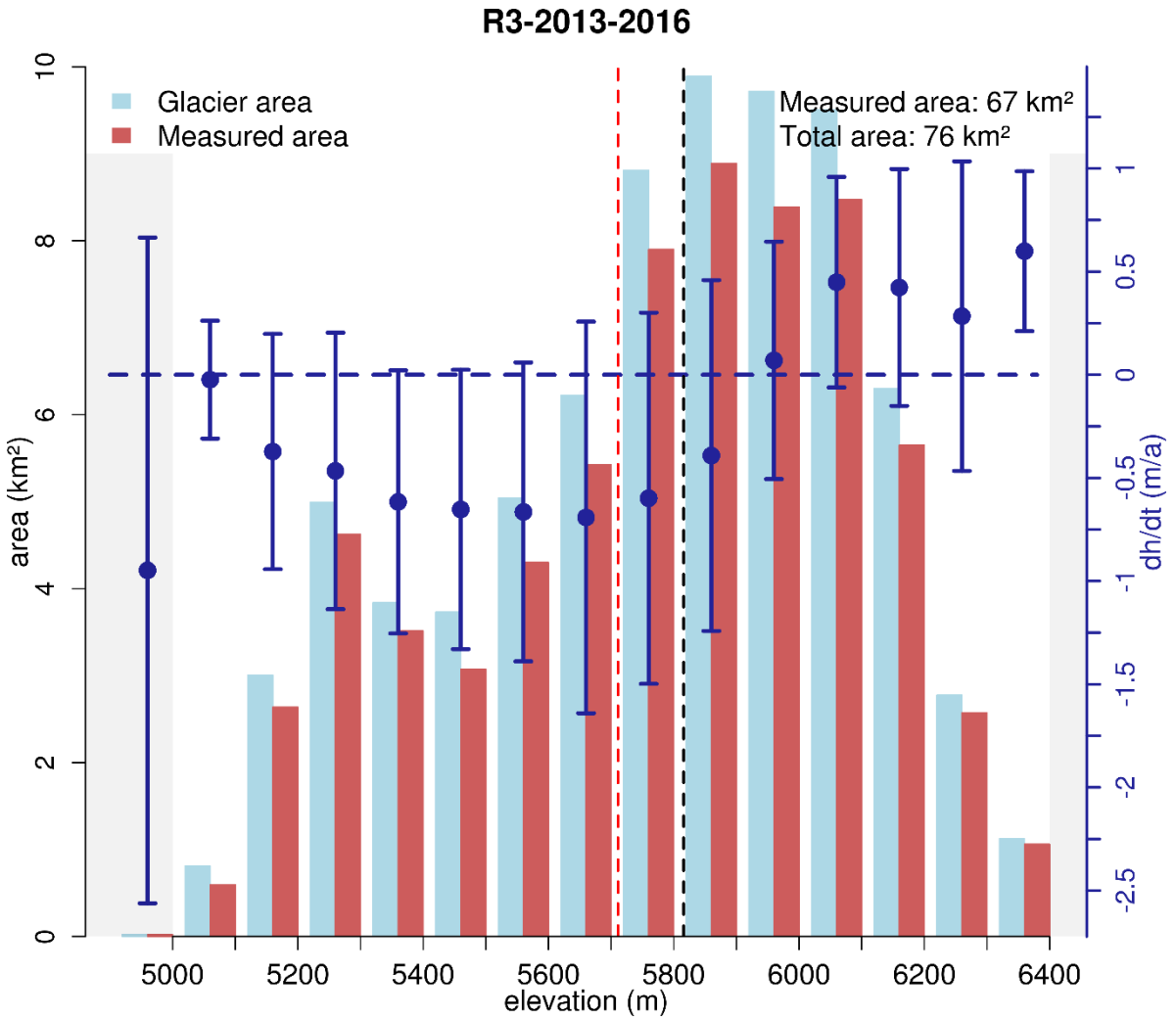

Figure S25. Hypsometric distribution of measured (red bars) and total (light blue bars) glacier area with elevation in subregion R3 in the interval 2013-2016. Blue dots represent the mean Δh/Δt value in each elevation interval. Error bars indicate NMAD of Δh/Δt for each hypsometric bin. Grey areas mark the lower and upper 1% quantile of the glacier area distribution. Black dashed line: mean glacier elevation; Red dashed line: equilibrium line altitude (ELA), see also Table S3. Area measurements are based on the glacier outlines from 2013, considering only regions with slopes below applied slope threshold (50°, see Section 4.2)

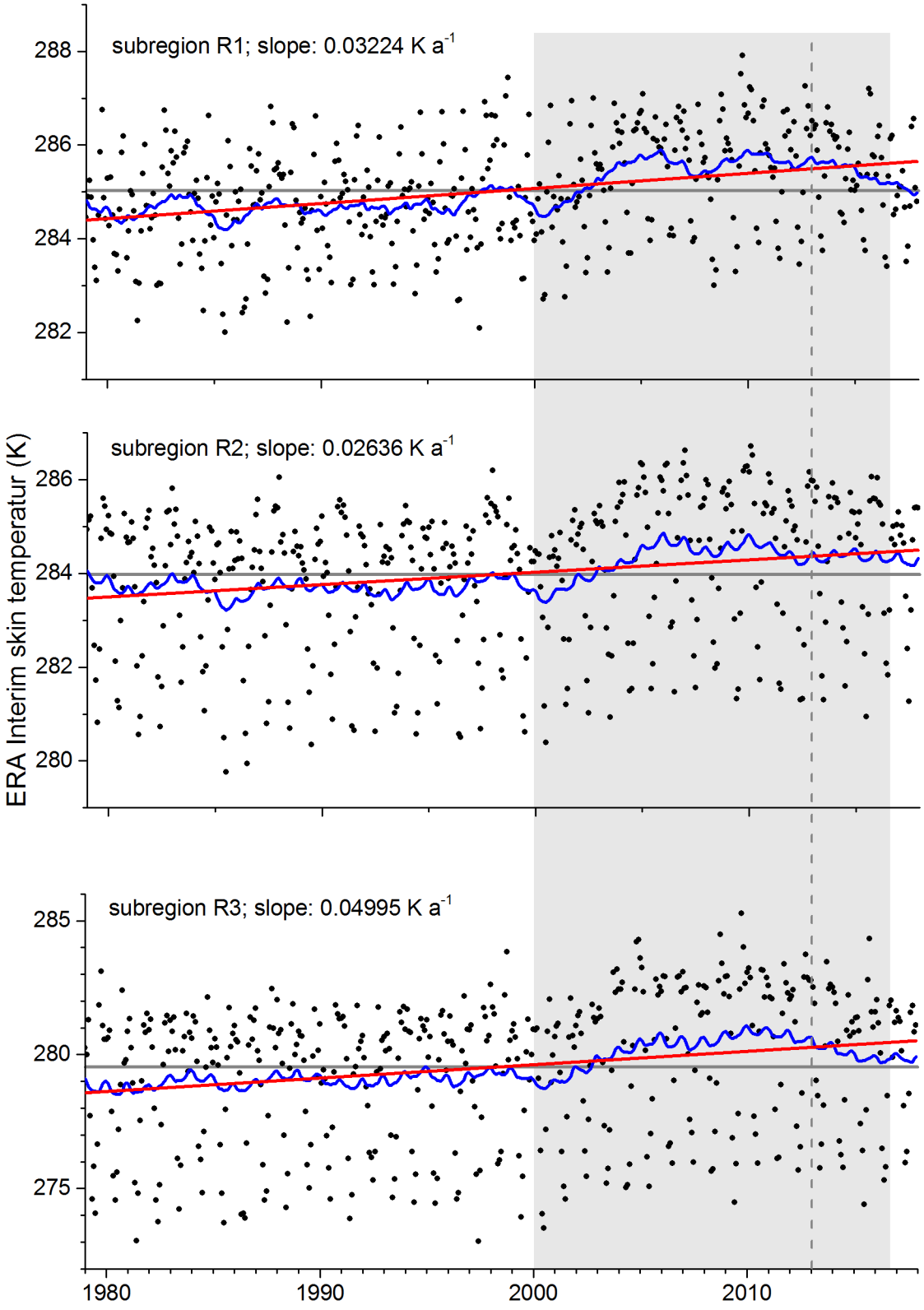

Figure S26. Skin temperature (monthly means of daily means) in the period 1979-2017 derived from ERA-Interim reanalysis data. Black dots: Spatial average values of glacier covered ERA-Interim grid cells in each subregion. Red line: long term trend (1979-2017), grey line: long term mean value; grey shaded area: period of mass budget and area change analysis, dashed grey line: marker for intermediate time step (early 2013)

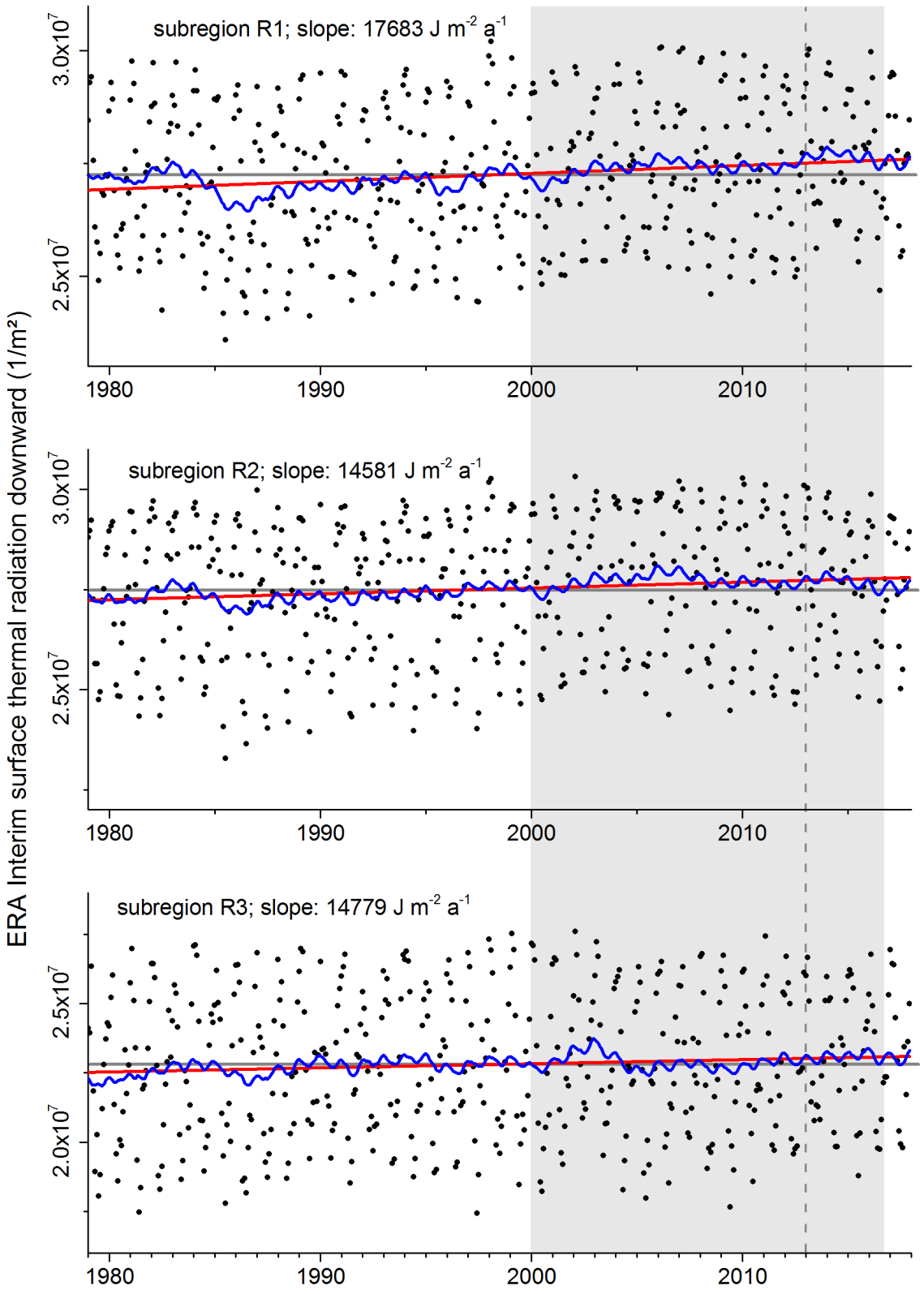

Figure S27. Surface thermal radiation downward (monthly means of daily forecast accumulations) in the period 1979-2017 derived from ERA-Interim reanalysis data. Black dots: Spatial average values of glacier covered ERA-Interim grid cells in each subregion. Red line: long term trend (1979-2017), grey line: long term mean value; grey shaded area: period of mass budget and area change analysis, dashed grey line: marker for intermediate time step (early 2013)

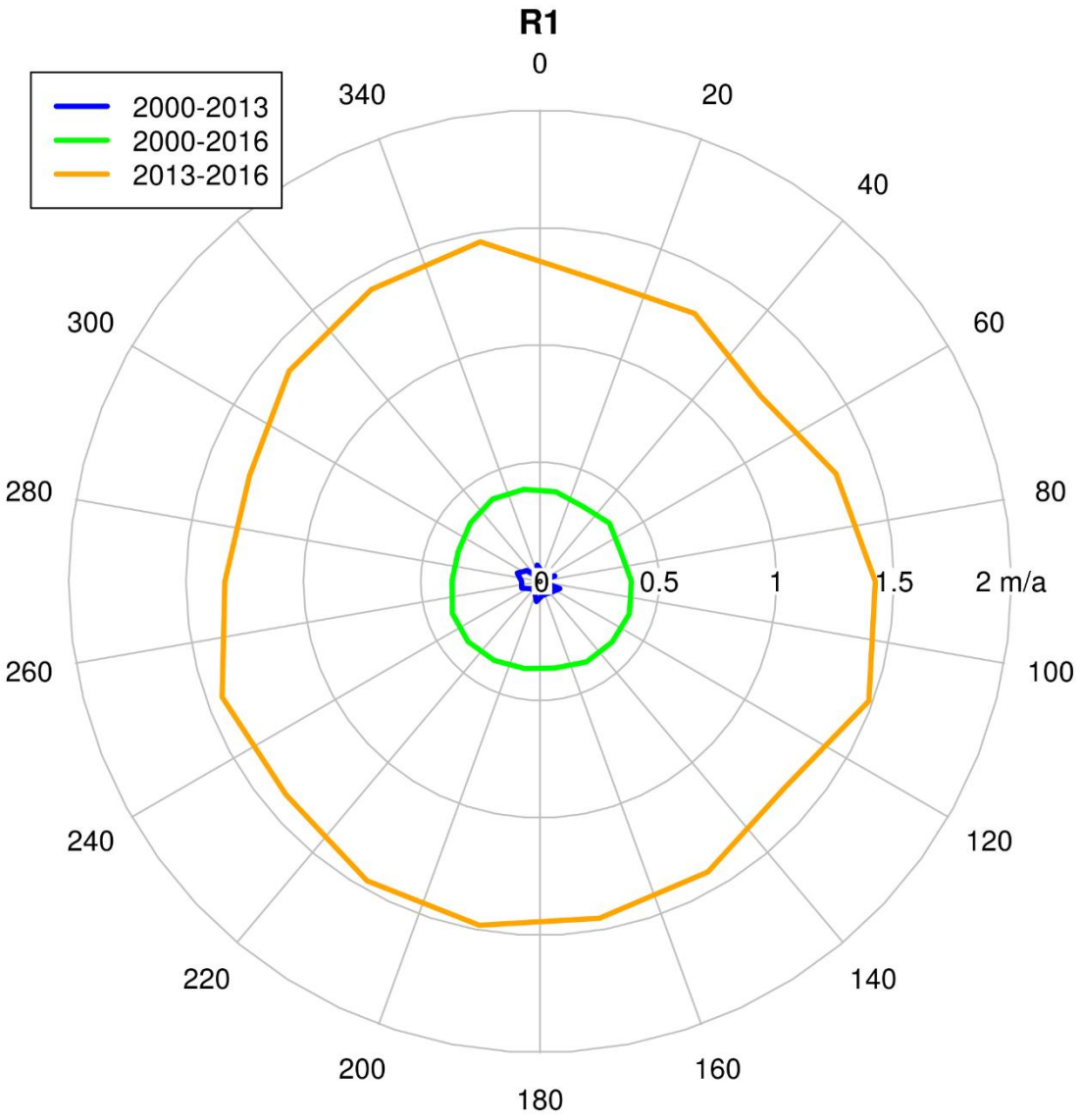

Figure S28. Polar plot of glacier surface lowering in subregion R1. The surface lowering measurements are averaged in aspect intervals of 20° (mean values).

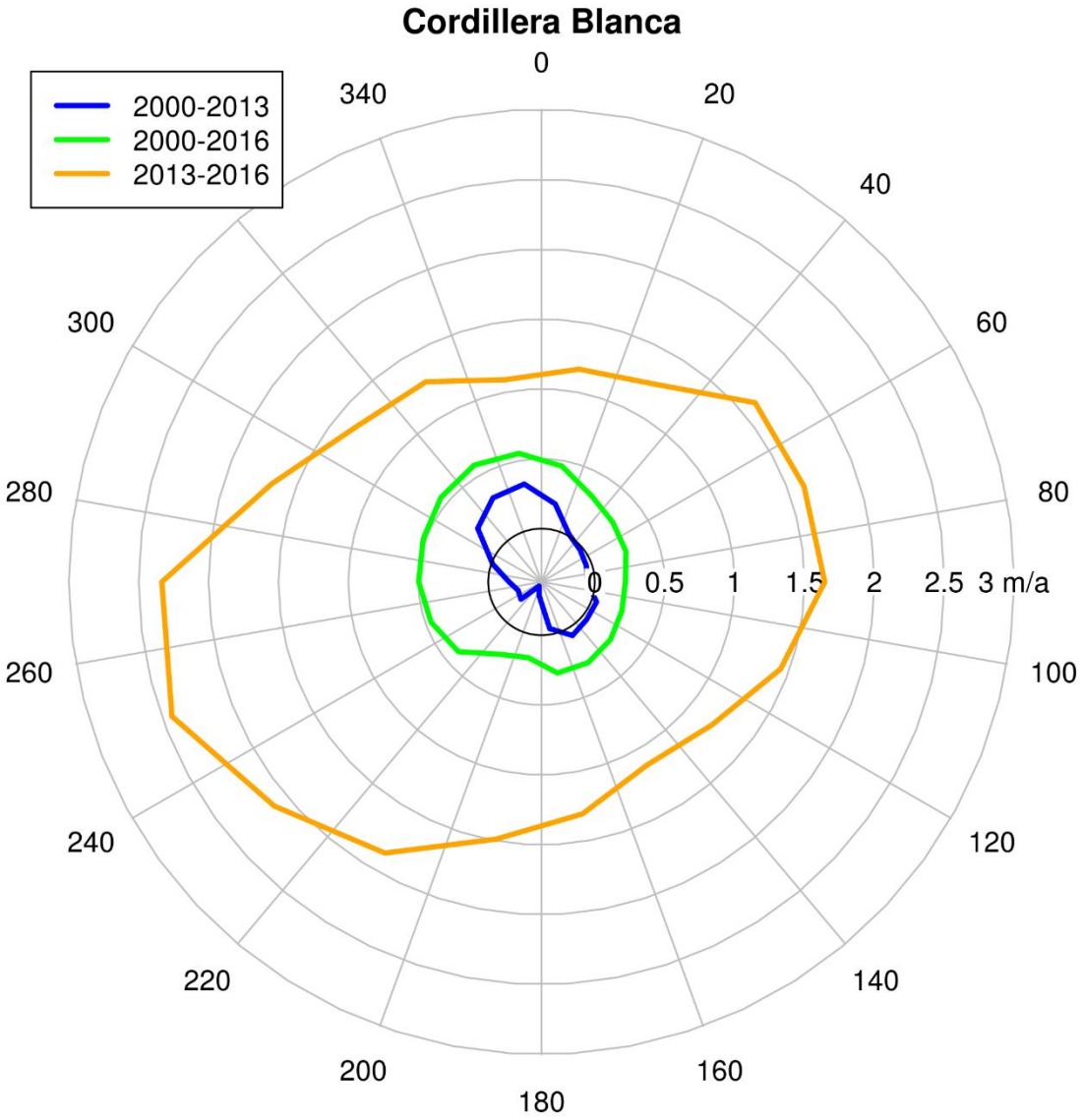

Figure S29. Polar plot of glacier surface lowering in Cordillera Blanca (subregion R1). The surface lowering measurements are averaged in aspect intervals of 20° (mean values).

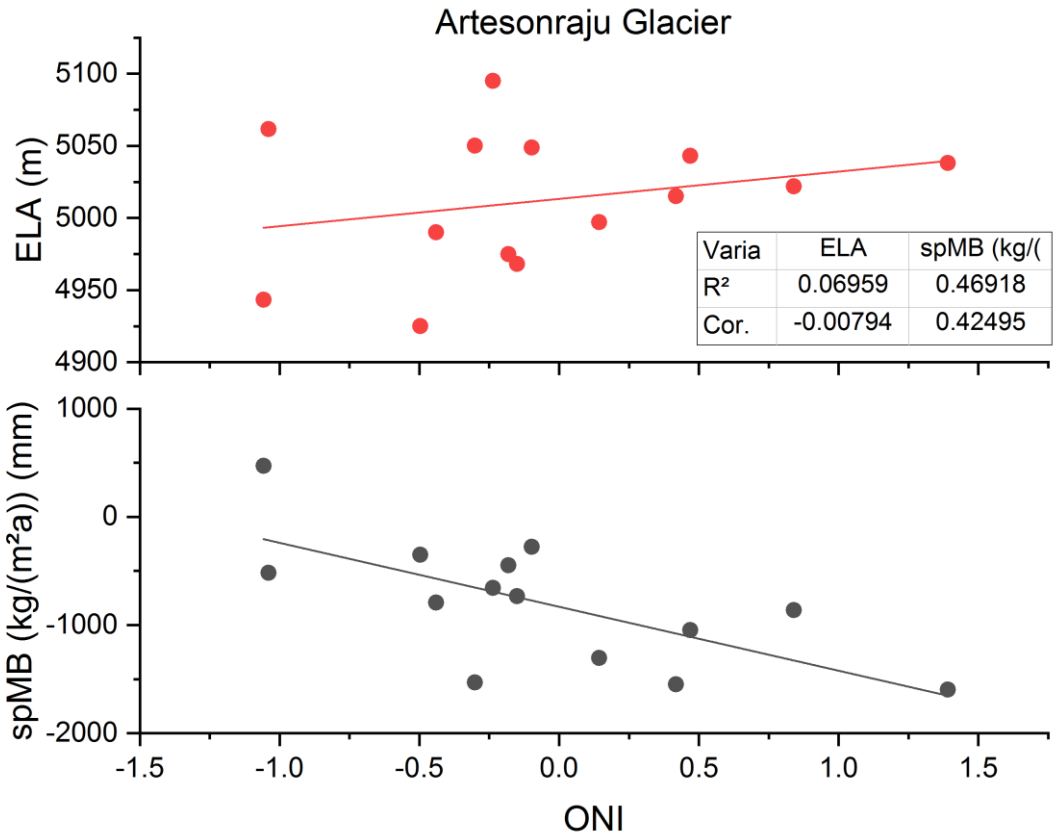

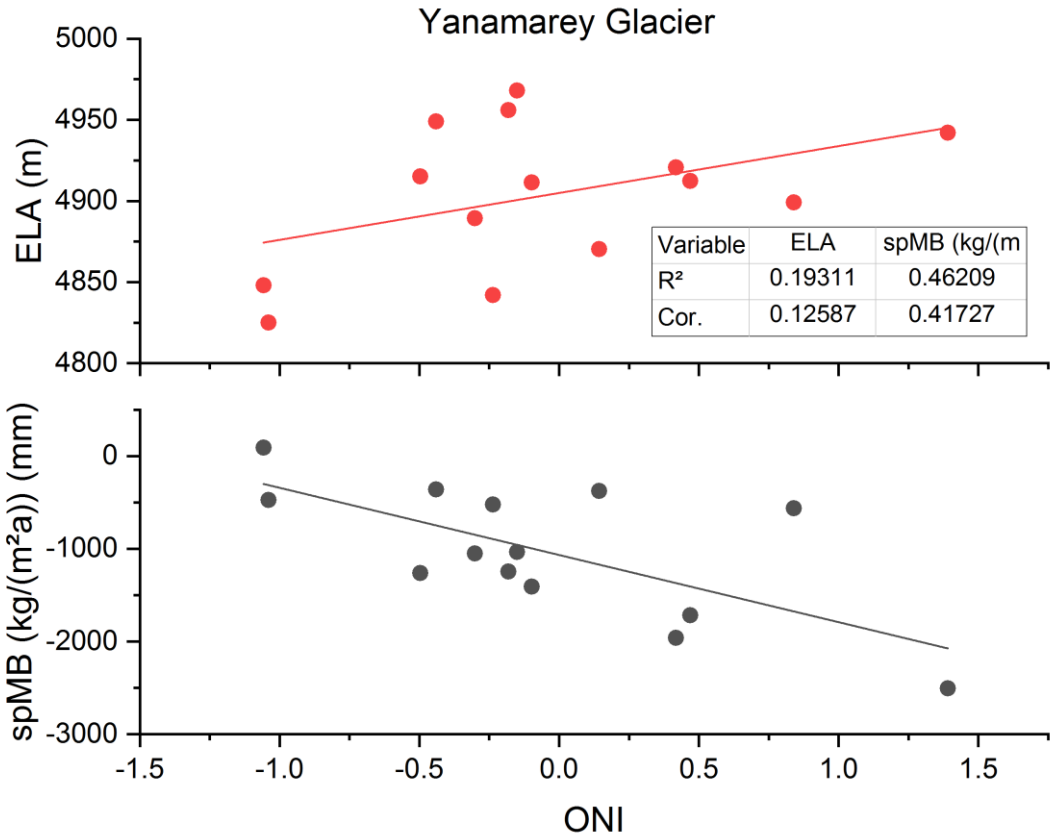

Figure S30. Annual equilibrium line altitude (ELA) and specific mass balance (spMB) derived from glaciological measurements plotted against average Oceanic Niño Index (ONI) of the respective observation periods (September-August) for Artesonraju and Yanamarey glaciers. Solid lines: linear fit of the respective variables.

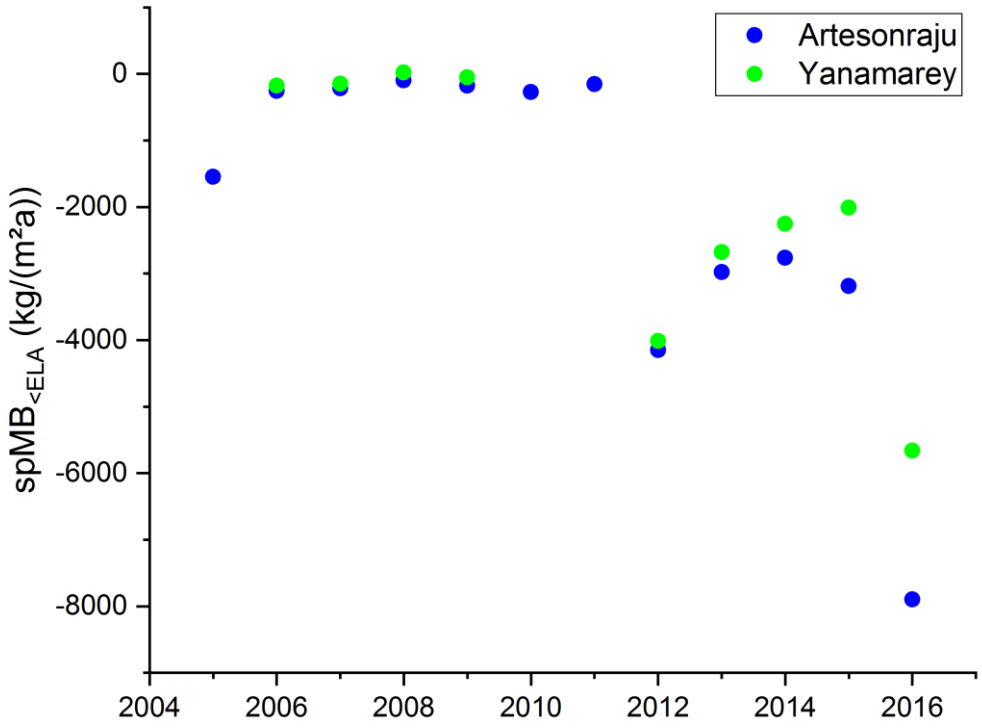

Figure S 31. Annual glaciological mass balance at regions below the ELA ($spMB_{<ELA}$) of Artesonraju and Yanamarey glaciers.

Table S1. Overview of analysed TanDEM-X imagery for elevation change analysis (continued on next pages)

date	path	strip	path direction*	images
Subregion: R1 northern wet outer tropics				
2011-12-04	081	70	D	1
2011-12-25	066	60	D	1
2012-01-05	066	50	D	3
2012-01-06	081	80	D	2
2012-01-11	157	70	D	1
2012-01-16	066	20	D	2
2012-01-22	157	10	D	1
2012-01-22	157	10	D	3
2012-01-22	157	10	D	1
2012-01-27	066	30	D	3
2012-02-02	157	60	D	4
2012-02-07	066	40	D	2
2012-02-13	157	80	D	2
2012-02-18	066	10	D	2
2012-02-24	157	50	D	4
2012-03-01	081	90	D	1
2012-03-06	157	90	D	1
2012-03-06	157	20	D	1
2012-03-12	081	80	D	1
2012-03-17	157	30	D	3
2012-03-22	066	60	D	2
2012-03-23	081	60	D	1
2012-03-28	157	40	D	2
2012-03-28	157	40	D	2
2012-12-30	028	85	A	4
2013-01-10	028	75	A	6
2013-01-14	081	85	D	6
2013-01-21	028	65	A	4
2013-01-24	066	45	D	2
2013-01-27	119	55	A	1
2013-01-30	157	65	D	1
2013-02-01	028	55	A	5
2013-02-04	066	55	D	2
2013-02-05	081	65	D	1
2013-02-10	157	45	D	2
2013-02-12	028	45	A	1
2013-02-15	066	25	D	2
2013-02-21	157	35	D	2
2013-02-26	066	15	D	1
2013-03-01	119	45	A	1
2013-03-04	157	25	D	1
2013-03-12	119	35	A	2
2013-03-15	157	15	D	5
2013-03-23	119	25	A	7
2013-03-26	157	05	D	6
2016-09-08	119	10	A	4
2016-09-13	028	50	A	2
2016-09-16	066	10	D	2
2016-09-19	119	20	A	1
2016-09-27	066	20	D	2
2016-09-30	119	30	A	2
2016-10-08	066	40	D	2
2016-10-11	119	40	A	5
2016-10-14	157	40	D	1
2016-10-16	028	90	A	5
2016-10-19	066	50	D	2
2016-10-22	119	50	A	1
2016-10-22	119	50	A	2
2016-10-25	157	50	D	1
2016-10-27	028	60	A	2
2016-11-02	119	60	A	2
2016-11-16	157	60	D	1
2016-12-08	157	80	D	2
2016-12-19	157	90	D	2

Subregion: R2 southern wet outer tropics				
2012-12-18	005	75	D	1
2012-12-29	005	65	D	1
2012-12-31	043	85	A	2
2013-01-04	096	75	D	3
2013-01-09	005	85	D	1
2013-01-10	020	75	D	2
2013-01-11	043	75	A	3
2013-01-15	096	65	D	1
2013-01-15	096	65	D	1
2013-01-17	134	85	A	3
2013-01-20	005	45	D	1
2013-01-22	043	65	A	1
2013-01-26	096	85	D	2
2013-01-28	134	75	A	2
2013-01-31	005	55	D	1
2013-02-01	020	85	D	2
2013-02-02	043	55	A	1
2013-02-06	096	45	D	1
2013-02-08	134	65	A	1
2013-02-13	043	45	A	1
2013-02-17	096	35	D	1
2013-02-19	134	55	A	2
2013-02-22	005	15	D	2
2013-02-24	043	35	A	2
2013-02-28	096	25	D	2
2013-03-02	134	45	A	1
2013-03-07	043	25	A	2
2013-03-11	096	15	D	2
2013-03-13	134	35	A	2
2013-03-16	005	05	D	2
2013-03-22	096	05	D	3
2013-03-24	134	25	A	3
2013-03-27	005	40	D	1
2013-04-02	096	70	D	1
2013-04-07	005	75	D	1
2013-04-18	005	10	D	2
2016-09-07	096	80	D	2
2016-09-09	134	20	A	2
2016-09-12	005	10	D	2
2016-09-13	020	90	D	1
2016-09-14	043	30	A	1
2016-09-18	096	10	D	1
2016-09-20	134	10	A	3
2016-09-29	096	20	D	1
2016-10-01	134	30	A	2
2016-10-04	005	40	D	1
2016-10-12	134	40	A	2
2016-10-15	005	50	D	1
2016-10-21	096	30	D	2
2016-10-23	134	50	A	3
2016-11-18	020	80	D	1
2016-11-28	005	60	D	1
2016-12-20	005	70	D	2
2016-12-26	096	70	D	2
Subregion: R3 dry outer tropics				
2012-12-02	096	15	D	1
2012-12-07	005	10	D	1
2012-12-29	005	65	D	1
2012-12-29	005	65	D	1
2012-12-31	043	85	A	1
2013-01-09	005	85	D	2
2013-01-11	043	75	A	4
2013-01-16	119	85	A	2
2013-01-20	005	45	D	3
2013-01-22	043	65	A	1
2013-01-22	043	65	A	2
2013-01-31	005	55	D	3
2013-02-02	043	55	A	2

2013-02-07	119	75	A	2
2013-02-13	043	45	A	4
2013-02-19	134	45	A	1
2013-02-24	043	35	A	3
2013-03-02	134	35	A	1
2013-03-07	043	25	A	2
2013-03-10	081	25	D	2
2013-03-13	134	25	A	2
2013-03-18	043	15	A	2
2013-03-21	081	15	D	2
2013-03-24	134	15	A	2
2013-04-02	096	70	D	2
2013-04-13	096	55	D	2
2013-04-24	096	45	D	2
2014-01-04	134	05	A	2
2014-01-15	134	15	A	2
2014-01-26	134	25	A	2
2014-03-09	096	50	D	2
2014-03-20	096	60	D	3
2016-09-07	096	10	D	1
2016-09-08	119	70	A	2
2016-09-09	134	10	A	2
2016-09-12	005	20	D	1
2016-09-14	043	20	A	1
2016-09-20	134	20	A	4
2016-09-23	005	30	D	2
2016-09-29	096	20	D	1
2016-09-30	119	80	A	1
2016-10-01	134	30	A	2
2016-10-04	005	40	D	2
2016-10-11	119	90	A	1
2016-10-12	134	40	A	1
2016-10-15	005	50	D	3
2016-10-21	096	30	D	2
2016-11-28	005	60	D	1
2016-12-26	096	80	D	1

*A – ascending, D – descending

Table S2. Overview of analysed Landsat imagery for glacier area mapping

Date	Path	row
Subregion: R1 northern wet outer tropic		
2000-09-09	6	68
2000-09-09	6	69
2000-08-15	7	67
2000-08-15	7	68
2000-07-21	8	66
2000-07-21	8	77
2013-06-16	7	67
2013-06-16	7	68
2013-07-09	8	66
2013-07-09	8	67
2013-07-11	6	68
2013-07-11	6	69
2013-08-19	7	67
2014-07-12	8	66
2014-07-12	8	67
2014-07-14	6	68
2014-08-22	7	67
2014-11-19	6	69
2014-11-26	7	68
2016-01-16	7	68
2016-01-16	7	69
2016-06-15	8	66
2016-06-15	8	67
2016-06-17	6	68
2016-07-10	7	67
Subregion: R2 southern wet outer tropic		
2000-06-23	4	69
2000-07-18	3	69
2000-07-18	3	70
2000-08-17	5	69
2000-08-28	2	70
2013-06-27	4	69
2013-06-29	2	70
2013-07-22	3	70
2014-06-05	5	69
2016-07-21	4	69
2016-07-23	2	70
2016-07-30	3	70
2016-08-29	5	69
Subregion: R3 dry outer tropics		
2000-07-25	4	70
2000-07-16	5	70
2000-08-03	3	71
2000-09-11	4	71
2000-09-13	2	71
2013-09-06	5	70
2013-09-08	3	71
2013-09-01	2	71
2013-09-15	4	70
2013-10-17	4	71
2016-05-11	3	71
2016-05-20	2	71
2016-07-28	5	70
2016-07-21	4	70
2016-07-21	4	71

Table S3: Snow line altitude (SLA) and equilibrium line altitude (ELA) reported for the study region and period. (RS: remote sensing, GL: glaciological method, AA: Area-Altitude method, H_{mean}: mean glacier elevation). Bold values indicate used average ELA for penetration depth bias estimation.

period	min (m a.s.l.)	max (m a.s.l.)	Type	Method	Source
Subregion R1					
2000-2015	4845	5085	SLA	RS	Veettil et al., 2017a
2000-2015	4720	4920	SLA	RS	Veettil et al., 2017b
1999-2005	5034	5086	SLA	RS	McFadden et al., 2011
2006-2010	4835	5075	SLA	RS	Lopez-Moreno et al., 2014
2006-2008	4953	4985	ELA	GL	Gurgiser et al., 2013
2004-2015	4959	5071	ELA	GL	Artesonraju Glacier, WGMS
2004-2015	4868	4942	ELA	GL	Yanamarey Glacier, WGMS
	average: 4955				
Subregion R2					
2000-2015	4680	5120	SLA	RS	Veettil et al., 2017b
1998-2009	5526	5414	SLA	RS	Hanshaw and Bookagen, 2014
1998-2016	5050	5414	ELA	H_{mean}	Drenkhan et al. 2018
	average: 5199				
Subregion R3					
2000-2014	5480	5745	SLA	RS	Veettil et al., 2016
2007	5910		ELA	AA	Ubeda, 2011
	average: 5711				

References:

Gurgiser, W., Marzeion, B., Nicholson, L., Ortner, M., Kaser, G., 2013. Modeling energy and mass balance of Shallap Glacier, Peru. The Cryosphere 7, 1787–1802. https://doi.org/10.5194/tc-7-1787-2013

Hanshaw, M.N., Bookhagen, B., 2014. Glacial areas, lake areas, and snow lines from 1975 to 2012: status of the Cordillera Vilcanota, including the Quelccaya Ice Cap, northern central Andes, Peru. The Cryosphere 8, 359–376. https://doi.org/10.5194/tc-8-359-2014

López-Moreno, J.I., Fontaneda, S., Bazo, J., Revuelto, J., Azorin-Molina, C., Valero-Garcés, B., Morán-Tejeda, E., Vicente-Serrano, S.M., Zubieta, R., Alejo-Cochachín, J., 2014. Recent glacier retreat and climate trends in Cordillera Huaytapallana, Peru. Glob. Planet. Change 112, 1–11. https://doi.org/10.1016/j.gloplacha.2013.10.010

McFadden, E.M., Ramage, J., Rodbell, D.T., 2011. Landsat TM and ETM+ derived snowline altitudes in the Cordillera Huayhuash and Cordillera Raura, Peru, 1986–2005. The Cryosphere 5, 419–430. https://doi.org/10.5194/tc-5-419-2011

Ubeda, J., 2011. El impacto del cambio climático en los glaciares del complejo volcánico Nevado Coropuna, (Cordillera Occidental de los Andes Centrales) (info:eu-repo/semantics/doctoralThesis). Universidad Complutense de Madrid, Servicio de Publicaciones, Madrid.

Veettil, B.K., Bremer, U.F., Souza, S.F. de, Maier, É.L.B., Simões, J.C., 2016. Variations in annual snowline and area of an ice-covered stratovolcano in the Cordillera Ampato, Peru, using remote sensing data (1986–2014). Geocarto Int. 31, 544–556. https://doi.org/10.1080/10106049.2015.1059902

Veettil, B.K., Wang, S., Bremer, U.F., de Souza, S.F., Simões, J.C., 2017a. Recent trends in annual snowline variations in the northern wet outer tropics: case studies from southern Cordillera Blanca, Peru. Theor. Appl. Climatol. 129, 213–227. https://doi.org/10.1007/s00704-016-1775-0

Veettil, B.K., Wang, S., Simões, J.C., Ruiz Pereira, S.F., de Souza, S.F., 2017b. Regional climate forcing and topographic influence on glacier shrinkage: eastern cordilleras of Peru. Int. J. Climatol. 38, 979–995. https://doi.org/10.1002/joc.5226